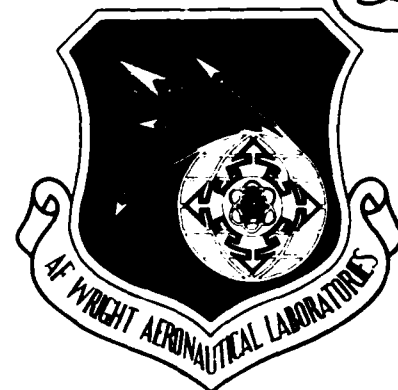


DTIC FILE COPY

2



AFWAL-TR-88-3109

AN EXPERIMENTAL EVALUATION OF THE AIR CANNON
TECHNIQUE FOR USE IN IMPACT RESISTANCE
SCREENING OF POLYCARBONATE

M. P. Bouchard

University of Dayton Research Institute
Dayton, Ohio 45469



Interim Report for Period October 1984 to February 1987

1989 February

Approved for Public Release; Distribution Unlimited

FLIGHT DYNAMICS LABORATORY
AIR FORCE WRIGHT AERONAUTICAL LABORATORIES
AIR FORCE SYSTEMS COMMAND
WRIGHT-PATTERSON AIR FORCE BASE, OHIO 45433-6553

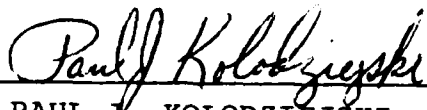
89 9 01 05 1

NOTICE

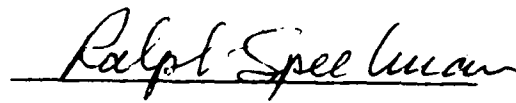
When Government drawings, specifications, or other data are used for any purpose other than in connection with a definitely related Government procurement operation, the United States Government thereby incurs no responsibility nor any obligation whatsoever; and the fact that the government may have formulated, furnished, or in any way supplied the said drawings, specifications, or other data, is not to be regarded by implication or otherwise as in any manner licensing the holder or any other person or corporation, or conveying any rights or permission to manufacture use, or sell any patented invention that may in any way be related thereto.

This report has been reviewed by the Office of Public Affairs (ASD/PA) and is releasable to the National Technical Information Service (NTIS). At NTIS, it will be available to the general public, including foreign nations.

This technical report has been reviewed and is approved for publication.



PAUL J. KOLODZIEJSKI, 1Lt, USAF
Aircraft Windshield Systems
Program Office
Vehicle Subsystems Division



RALPH J. SPEELMAN, Chief
Aircraft Windshield Systems
Program Office
Vehicle Subsystems Division

FOR THE COMMANDER



RICHARD E. COLCLOUGH, JR.
Chief
Vehicle Subsystems Division

If your address has changed, if you wish to be removed from our mailing list, or if the addressee is no longer employed by your organization please notify WRDC/FIVRC, W-PAFB, OH 45433 to help us maintain a current mailing list.

Copies of this report should not be returned unless return is required by security considerations, contractual obligations, or notice on a specific document.

UNCLASSIFIED

SECURITY CLASSIFICATION OF THIS PAGE

REPORT DOCUMENTATION PAGE

Form Approved
OMB No. 0704-0188

1a. REPORT SECURITY CLASSIFICATION Unclassified			1b. RESTRICTIVE MARKINGS			
2a. SECURITY CLASSIFICATION AUTHORITY			3. DISTRIBUTION/AVAILABILITY OF REPORT Approved for public release; distribution unlimited			
2b. DECLASSIFICATION/DOWNGRADING SCHEDULE						
4. PERFORMING ORGANIZATION REPORT NUMBER(S) UDR-TR-87-15			5. MONITORING ORGANIZATION REPORT NUMBER(S) AFWAL-TR-88-3109			
6a. NAME OF PERFORMING ORGANIZATION University of Dayton Research Institute		6b. OFFICE SYMBOL (if applicable)		7a. NAME OF MONITORING ORGANIZATION Air Force Wright Aeronautics Lab. Flight Dynamics Laboratory (AFWAL/FDER)		
6c. ADDRESS (City, State, and ZIP Code) 300 College Park Dayton, Ohio 45469			7b. ADDRESS (City, State, and ZIP Code) Wright-Patterson AFB, OH 45433-6553			
8a. NAME OF FUNDING/SPONSORING ORGANIZATION		8b. OFFICE SYMBOL (if applicable)		9. PROCUREMENT INSTRUMENT IDENTIFICATION NUMBER F33615-84-C-3404		
8c. ADDRESS (City, State, and ZIP Code)			10. SOURCE OF FUNDING NUMBERS			
			PROGRAM ELEMENT NO.	PROJECT NO.	TASK NO.	WORK UNIT ACCESSION NO.
			64212F	1926	01	12
11. TITLE (Include Security Classification) AN EXPERIMENTAL EVALUATION OF THE AIR CANNON TECHNIQUE FOR USE IN IMPACT RESISTANCE SCREENING OF POLYCARBONATE						
12. PERSONAL AUTHOR(S) M. P. Bouchard						
13a. TYPE OF REPORT Interim		13b. TIME COVERED FROM 84OCT TO 87FEB		14. DATE OF REPORT (Year, Month, Day) 1989 February		15. PAGE COUNT 82
16. SUPPLEMENTARY NOTATION						
17. COSATI CODES			18. SUBJECT TERMS (Continue on reverse if necessary and identify by block number)			
FIELD	GROUP	SUB-GROUP	polycarbonate, air cannon, Projectile,			
01	03		Falling weight, impact resistance, strain rate,			
			accelerated impactor, Lexan, AIRCRAFT, ARMOR. (YES)			
19. ABSTRACT (Continue on reverse if necessary and identify by block number) An evaluation of the air cannon test technique for impact resistance screening of polycarbonate was conducted. Tests were performed on plate specimens of various spans and thicknesses impacted by projectiles of various diameters, masses, and velocities. Strain rate, failure energy, failure mode, and percent thickness reduction were recorded. Falling weight tests were also conducted and results compared with the air cannon results. The air cannon results showed the same trends in the failure energy-versus-geometric parameter and in failure mode as the falling weight results. The air cannon test technique yielded strain rates characteristic of birdstrike for both thin (1/8 inch) and thick (1/2 inch) plates while the falling weight test achieved such strain rates only for thin (1/8 inch) plates. The air cannon technique is therefore the test of choice when strain rate is critical. When strain rate is not critical, the falling weight test is the method of choice because of its low testing and maintenance costs. Further air cannon testing should be conducted to refine some of the findings, especially in regard to the nonlinear dependence of failure energy on projectile velocity (mass).						
20. DISTRIBUTION/AVAILABILITY OF ABSTRACT <input checked="" type="checkbox"/> UNCLASSIFIED/UNLIMITED <input type="checkbox"/> SAME AS RPT. <input type="checkbox"/> DTIC USERS			21. ABSTRACT SECURITY CLASSIFICATION Unclassified			
22a. NAME OF RESPONSIBLE INDIVIDUAL Lt Paul J. Kolodziejewski			22b. TELEPHONE (Include Area Code) (513) 255-2916		22c. OFFICE SYMBOL AFWAL/FDER	

FOREWORD

The effort reported herein was performed by the University of Dayton Research Institute, Dayton, Ohio, under Contract No. F33615-84-C-3404, "Birdstrike Resistant Crew Enclosure Development Program." This work was administered by the Air Force Flight Dynamics Laboratory, Wright-Patterson Air Force Base, Ohio, with administrative direction provided by Lt. Donato Altobelli, AFWAL/FIEA.

Project supervision and technical assistance was provided through the Aerospace Mechanics Division of the University of Dayton Research Institute with Mr. Dale H. Whitford, Supervisor, and Mr. Blaine S. West, Head, Applied Mechanics Group and Project Engineer. Mr. Michael P. Bouchard served as Principal Investigator. The following persons are gratefully acknowledged for their contributions to this project: Mr. Henry Williams, Mr. Charles Acton, and Mr. Robert Bertke of the Impact Physics Group for performing the accelerated impactor tests; Mr. R. David Kemp of the Applied Mechanics Group for performing the falling weight tests; Mr. Fred Pestian, Mr. Jim Higgins, and Mr. Rick Dubell of the Machine Shop for fabricating specimens and projectiles and for performing specimen thickness measurements; Mr. Stephen Bless of the Impact Physics Group for providing technical information concerning ballistic testing; Mr. Greg Stenger of the Applied Mechanics Group for providing helpful insight and advice throughout the effort; and Mrs. Rita Tudor and Mrs. Mary Wright for typing the manuscript, especially the lengthy tables.

Accession For	
NTIS CRA&I	<input checked="" type="checkbox"/>
DTIC TAB	<input type="checkbox"/>
Unannounced	<input type="checkbox"/>
Justification	
By	
Distribution /	
Availability Codes	
Dist	Avail and/or Special
A-1	




TABLE OF CONTENTS

SECTION	PAGE
1 INTRODUCTION	1
1.1 Background	1
1.2 Objectives	2
1.3 Approach	2
2 TEST PROGRAM	4
2.1 Test Specimens	4
2.2 Air Cannon Test Setup	5
2.3 Air Cannon Test Procedure	16
2.4 Falling Weight Test Setup	22
2.5 Falling Weight Test Procedure	22
3 RESULTS	27
3.1 Air Cannon Test Results	27
3.2 Falling Weight Test Results	27
3.3 Discussion and Comparison of Results	27
3.3.1 Strain Rates	27
3.3.2 Failure Energy	32
3.3.3 Failure Mode	41
3.3.4 Percent Reduction in Thickness	52
4 CONCLUSIONS	56
5 RECOMMENDATIONS	58
REFERENCES	60
APPENDIX A: Computation of Specimen Strain Rates	A-1
A. Introduction	A-2
B. Nomenclature	A-2
C. Strain Rate Derivation	A-3
D. Strain Rate Results	A-7
APPENDIX B: Summary of Air Cannon Test Data	B-1
APPENDIX C: Summary of Falling Weight Test Data	C-1

LIST OF ILLUSTRATIONS

FIGURE	PAGE
2.1 Specimen Layout for 0.125-inch Polycarbonate Sheet	6
2.2 Specimen Layout for 0.25-inch Polycarbonate Sheet	7
2.3 Specimen Layout for 0.5-inch Polycarbonate Sheet No. 1	8
2.4 Specimen Layout for 0.5-inch Polycarbonate Sheet No. 2	9
2.5 Specimen Layout for 0.5 inch Polycarbonate Sheet No. 3	10
2.6 Specimen Layout for 0.75-inch Polycarbonate Sheet	11
2.7 Air Cannon Test Setup	12
2.8 Support Frame for Air Cannon Test Setup	14
2.9 Projectiles for Air Cannon Tests	15
2.10 Typical Sabot Before and After Modification	17
2.11 Typical Threshold of Failure Crack	21
2.12 Falling Weight Test Apparatus for Plate Specimens	23
3.1 Comparison of Failure Energy versus Plate Span for Similar Air Cannon and Falling Weight Tests	33
3.2 Comparison of Failure Energy versus Plate Thickness for Similar Air Cannon and Falling Weight Tests	34
3.3 Comparison of Failure Energy versus Projectile Diameter for Similar Air Cannon and Falling Weight Tests	35
3.4 Variation of Failure Energy with Projectile Velocity for Various Plate Spans	37

LIST OF ILLUSTRATIONS (continued)

FIGURE	PAGE
3.5 Variation of Failure Energy with Projectile Mass for Various Plate Spans	38
3.6 Ballistic Limit (Specimen M-6)	43
3.7 Comparison of Overall Plate Bending for Similar Air Cannon and Falling Weight Specimens	44
3.8 Typical Petalling (Bending) Specimens	45
3.9 Typical Cupping (Tensile) Failure	47
3.10 Typical Plugging (Shear) Failure	48

LIST OF TABLES

TABLE	PAGE
2.1 Air Cannon Test Matrix Arranged by Specimen Group	18
2.2 Air Cannon Test Matrix Arranged by Test Variable	19
2.3 Falling Weight Test Matrix Arranged by Specimen Group	24
2.4 Falling Weight Test Matrix Arranged by Test Variable	26
3.1 Air Cannon Test Results Summarized by Specimen Group	28
3.2 Air Cannon Test Results Summarized by Test Variable	29
3.3 Falling Weight Test Results Summarized by Test Group	30
3.4 Falling Weight Test Results Summarized by Test Variable	31
3.5 Comparison of Air Cannon and Falling Weight Failure Modes versus Geometric Test Variable	49
3.6 Comparison of Air Cannon and Falling Weight Failure Modes versus Projectile Velocity	51
3.7 Comparison of Air Cannon and Falling Weight Percent Thickness Reduction versus Geometric Test Variable	53
3.8 Comparison of Air Cannon and Falling Weight Percent Thickness Reduction versus Projectile Velocity	54

SECTION 1

INTRODUCTION

1.1 BACKGROUND

High performance United States Air Force Aircraft are being fitted with transparencies utilizing polycarbonate (MIL-P-83310) material as the structural ply. Polycarbonate offers many advantages as a structural transparency material, having excellent impact (e.g., birdstrike) resistance as well as acceptable optical and thermal properties. Polycarbonate impact resistance is influenced by a variety of parameters including thickness, temperature, ply configuration, processing procedures, surface finish, aging, and environmental exposure. In order to optimize the impact resistance of a candidate transparency design, the transparency designer must be able to evaluate the effect of these parameters.

Several test techniques exist for evaluating the impact resistance of polycarbonate, including the falling weight, notched Izod, notched Charpy, high rate flexure, high rate tension, and air cannon techniques. Reference 2 briefly discusses and compares these techniques (including methods, equipment, capabilities, and costs). The air cannon technique is the subject of the present report. A projectile is propelled by a compressed gas or powder charge through a gun barrel into the specimen. Projectile velocities of up to 3,000 ft/sec are possible for the 1.5-inch-bore cannon installed at the UDRI Impact Physics Gun Range^{2,10} used in the present investigation.

One potential advantage of the air cannon technique is that high specimen strain rates can be achieved (up to 10,000 in/in/sec for the UDRI 1.5-inch cannon²). Peak strain rates of 100-450 in/in/sec have been computed by UDRI from a limited

number of high-speed films of birdstrike tests on T-38 and F-111 windshields. Reference 3 cites birdstrike induced strain rates of 30-200 in/in/sec. In addition, tensile testing of polycarbonate has demonstrated that the polycarbonate material properties are strain rate dependent.⁴ With the air cannon test technique the potential therefore exists for performing impact screening of polycarbonate specimens at strain rates characteristic of birdstrike. The program documented herein was initiated to evaluate the use of the air cannon test in determining polycarbonate impact resistances.

1.2 OBJECTIVES

The objectives of this test program were:

1. Collect data to show the effects of various test parameters on air cannon test results.
2. Compare air cannon test results and trends with falling weight test results and trends (the falling weight test technique is an ASTM standard test method^{1,2} for impact resistance testing of polycarbonate).

1.3 APPROACH

Air cannon tests were performed and the following test results recorded: strain rate, failure energy, percent reduction in plate thickness, and failure mode. The test results were then correlated with changes in the test parameters. This correlation was performed to determine the effects of changing a single test parameter (such as plate span/thickness/boundary conditions and projectile diameter/mass/velocity) on the test results. From this correlation, test result-versus-test parameter trends were obtained.

Finally, air cannon test results and trends were correlated with falling weight test results and trends. Significant differences in the results/trends due to the high strain rates (typical of birdstrike) associated with the air cannon test would mean that the air cannon test would be better suited for impact resistance screening of polycarbonate in terms of achieving the strain rate effects associated with birdstrike. Some falling weight data was already available for comparison; additional data needed for determining falling weight result-parameter trends was obtained by performing the needed falling weight tests.

SECTION 2

TEST PROGRAM

2.1 TEST SPECIMENS

The test specimens were square plates bandsawed from new General Electric 9030 series commercial-grade Lexan sheet. Commercial grade Lexan was used because: (1) its impact resistance is similar to that of MIL-specification polycarbonate²; (2) the cost is lower and the material more readily available than MIL-specification polycarbonate; and (3) a direct comparison of results with those of a previous test program² which used 9030 Lexan was needed. (The basic difference between MIL-SPEC and commercial grade polycarbonate is the optical quality. MIL-SPEC material contains fewer inclusions, i.e., trapped particles, and had no added color, resulting in better optical quality.) Nominal sheet/specimen thicknesses were 1/8 in., 1/4 in., 1/2 in., and 3/4 in., corresponding to actual (measured) thicknesses of 0.115 in., 0.225 in., 0.45 in., and 0.81 in. The plate dimensions were 2 inches greater than the test span so that edge effects from sawing were negligible and so that adequate material was available for clamping for fixed-edge boundary conditions. The test spans were 4, 5, 8, and 10 inches, so that the corresponding specimen sizes were 6 in. by 6 in., 7 in. by 7 in., 10 in. by 10 in., and 12 in. by 12 in. Seven replicates were fabricated for each test result that was to be obtained.

An identifying code was engraved near the edge of each specimen. For the air cannon specimens the code was of the form "X-YY", where "X" was a letter indicating the test group (A-W) and "YY" was a two-digit identifier (01-07) to distinguish samples within the same test group. The code for falling weight specimens consisted of the letter "F" for falling weight followed

by a code of the form "X-YY", where "X" was a letter indicating the test group (A-I) and "YY" was a two-digit identifier (01-07) to distinguish samples within the same test group.

Figures 2.1 - 2.6 are drawings showing each specimen in its parent sheet.

2.2 AIR CANNON TEST SETUP

Figure 2.7 shows the air cannon test setup. A 6-foot long, 1.5-inch bore (inside diameter), thick-walled steel tube, supported on a heavy I-beam, served as the gun barrel. The propellant was either compressed helium (100-500 psi) for lower velocities (100-250 ft/sec) or Bullseye gun powder for higher velocities (250-1100 ft/sec). A vent section attached to the end of the gun barrel released driving pressure from the rear of the projectile package as it left the barrel.

Projectiles were placed in a polycarbonate sabot (carrier) for launching. The sabots were 1.5-inch-outside diameter cylinders, with the inside machined to hold the projectile. The sabots were stripped from the projectiles in the stripper section of the gun to keep the sabot from traveling on into the test specimen. The stripper section had a gradually tapering inside diameter which "pinched" the sabot, decelerating it to a stop while allowing the projectile to continue on trajectory to the target.

Between the launcher and target the projectiles passed through two laser beams which triggered on, and then off, an electronic timer. Because the lasers were spaced a known distance apart, projectile velocity was computed as the laser spacing divided by the elapsed time between the lasers.

After passing through the lasers, the projectiles progressed on into the test specimen. A "picture frame" fixture

Scale: 1 inch = 1 foot

F1	F2	F3	F4	F5	F6	F7	
----	----	----	----	----	----	----	--

FC-1	FC-2	FC-3	FC-4	FC-5	FC-6
FC-7	FG-1	FG-2	FG-3	FG-4	FG-5
FG-6	FG-7	FH-1	FH-2	FH-3	FH-4
FH-5	FH-6	FH-7	FI-1	FI-2	FI-3
FI-4	FI-5	FI-6	FI-7	Spare 1	Spare 2

Figure 2.1. Specimen Layout for 0.125-inch Polycarbonate Sheet.

Scale: 1 inch = 1 foot

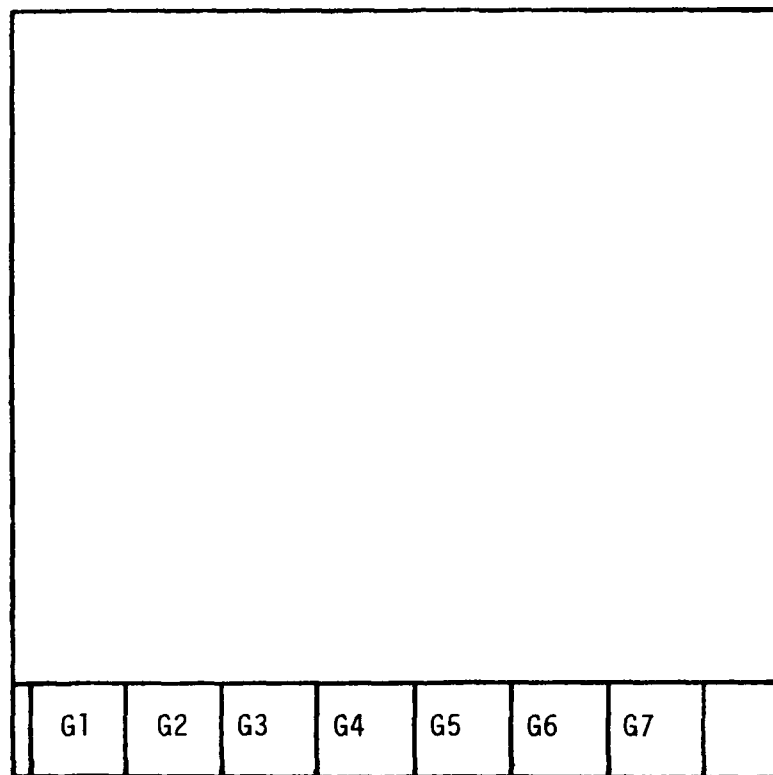


Figure 2.2. Specimen Layout for 0.25-inch Polycarbonate Sheet.

Scale: 1 inch = 1 foot

Spare	K1	J4	J3	I3	I2	H2	H1	D1	L1	B4	A4
K7	K2	J5	J2	I4	I1	H3	D7	D2	L2	B3	A3
K6	K3	J6	J1	I5	H7	H4	D6	D3	L3	B2	A2
K5	K4	J7	I7	K6	H6	H5	D5	D4	L4	B1	A1
Spare	Spare	Spare	Spare	Spare	Spare	Spare	Spare	Spare			
E1	E2	E3	E4	E5	E6	E7					

Figure 2.3. Specimen Layout for 0.5-inch Polycarbonate Sheet No. 1.

Scale: 1 inch = 1 foot

R1	R2	R3	R4	R5	U1	U2	U3	FB1
R6	R7	S1	S2	S3	U4	U5	U6	FB2
S4	S5	S6	S7	T1	U7	V1	V2	FB3
T2	T3	T4	T5	T6	V3	V4	V5	FB4
								FB5
								FB6
								FB7
					FD1	FD2	FD3	
							FD4	

Figure 2.4. Specimen Layout for 0.5-inch Polycarbonate Sheet No. 2.

[illegible]

Figure 2.5. Specimen Layout for 0.5-inch Polycarbonate Sheet No. 3.

Scale: 1 inch = 1 foot

01	05	
02	06	
03	07	
04	Spare	

Figure 2.6. Specimen Layout for 0.75-inch Polycarbonate Sheet.



Figure 2.7. Air Cannon Test Setup.

with a 10-inch square opening was used to support the specimens. The frame was fabricated from a heavy (6-inch-deep) steel I-beam for rigidity. Specimens to be simply supported were taped onto the front of the frame (i.e., the side facing the oncoming projectile). Specimens to be clamped around their perimeters were sandwiched between two annular, 1-inch-thick aluminum plates, giving circular openings of 4, 5, or 8-inch diameters depending on which set of plates was used. The annular plates were the same ones used for supporting falling weight test specimens. The sandwich assembly was bolted and C-clamped to the I-beam frame as shown in Figure 2.8. The specimen support fixturing was housed inside a steel box to contain the projectiles in case of ricochet off of or penetration through the specimens.

Seven different projectile types were used for the tests, as shown in Figure 2.9. The projectiles were designed to test the effects of varying nose diameter, holding mass constant, and of varying mass, holding nose diameter constant. All projectiles had hemispherically shaped noses.

The Type 1 projectile was a commercially available steel ball bearing. The Type 2 - Type 7 projectiles were turned on a lathe to the geometries shown. The Type 2,3,5,6, and 7 projectiles were fabricated from AISI O1 steel and hardened to R_c 47-50. The Type 4 projectile was fabricated from 6061-T6 aluminum to achieve the desired mass. Two replicates of each projectile type were fabricated except for Type 4. Seven Type 4 replicates, one for each shot, were fabricated since the relatively soft aluminum was expected to permanently deform on impact, making a projectile unusable for subsequent shots. The surface finish of the machined projectiles was approximately 80 μ in.



Figure 2.8. Support Frame for Air Cannon Test Setup.

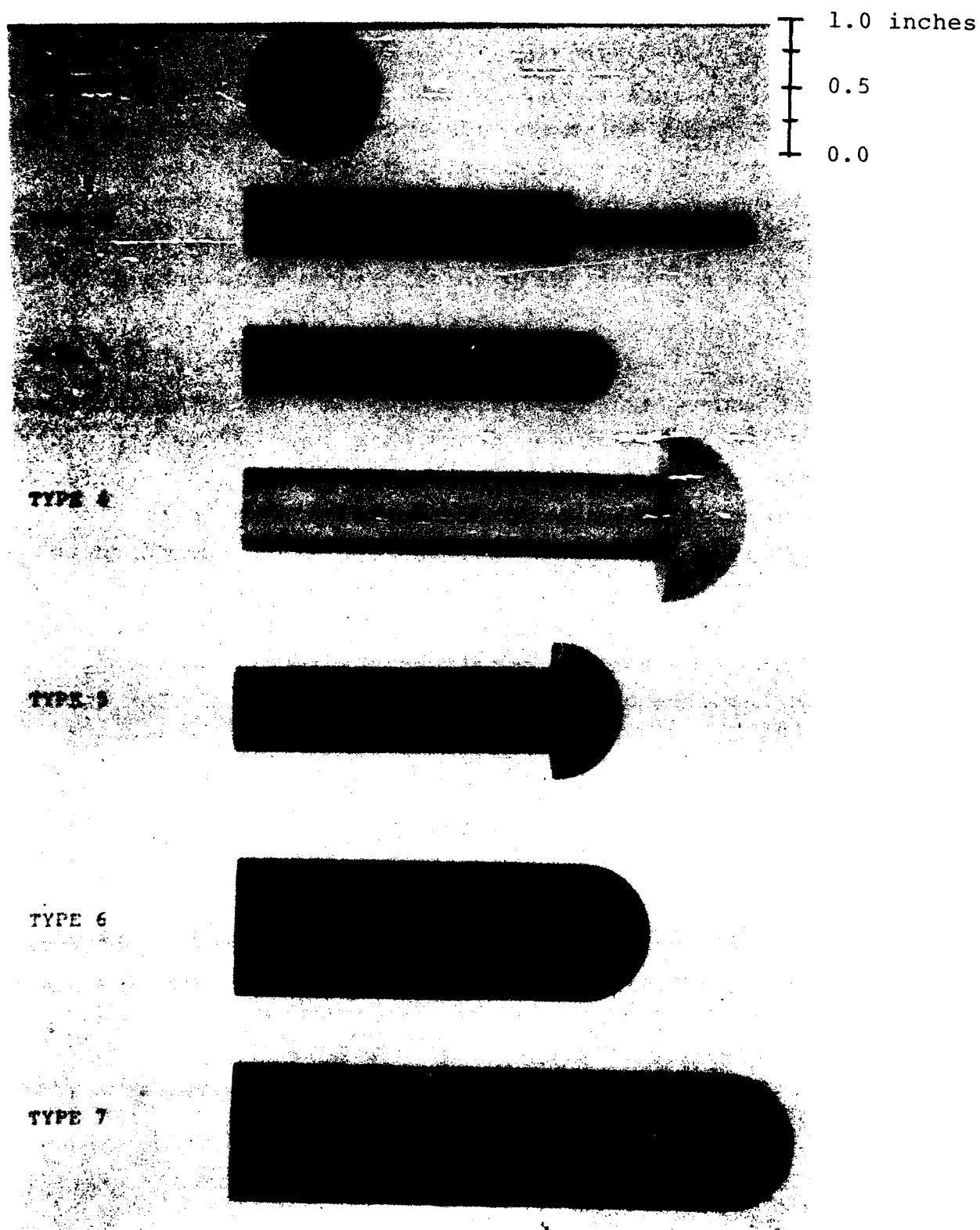


Figure 2.9. Projectiles for Air Cannon Tests.

The geometry of several of the impactor types deviated from the simple constant-diameter cylindrical shape. The Type 4 and 5 impactors were "mushroom" shaped to achieve a desired nose diameter while maintaining a desired mass and a length-to-diameter ratio that would provide stable flight (typically 2:1 or more). The Type 2 impactor consisted of two pieces - a nose and a sleeve. This construction provided for easier removal of the projectile if it became imbedded in a specimen and allowed for replacement of the relatively long, slender nose should it buckle during impact.

The initial sabot geometries were designed so that the projectiles had 0.013-inch radial clearance with the inner sabot wall. During testing it was found that some of the projectile types tended to tumble toward their targets due to interference with the sabot walls during the sabot stripping portion of the shot. The inside sabot diameter was therefore increased to provide 0.025 - 0.030 inch of radial clearance. In addition, the outside diameter was reduced to approximately 1.35 inches (from 1.50 inches) along the front half of the sabot to prevent pinching of the front end of the sabot by the sabot stripper. Typical standard and modified sabots are shown in Figure 2.10.

2.3 AIR CANNON TEST PROCEDURE

Table 2.1 presents the air cannon test matrix. Twenty-three sets of seven tests each were performed, for a total of 161 tests. Several test parameters were varied to determine their effects on the results. These parameters included plate thickness and span; specimen edge fixity; and projectile diameter and mass (velocity). Table 2.2 is a re-arrangement of Table 2.1 showing the test sets used to investigate each test parameter.

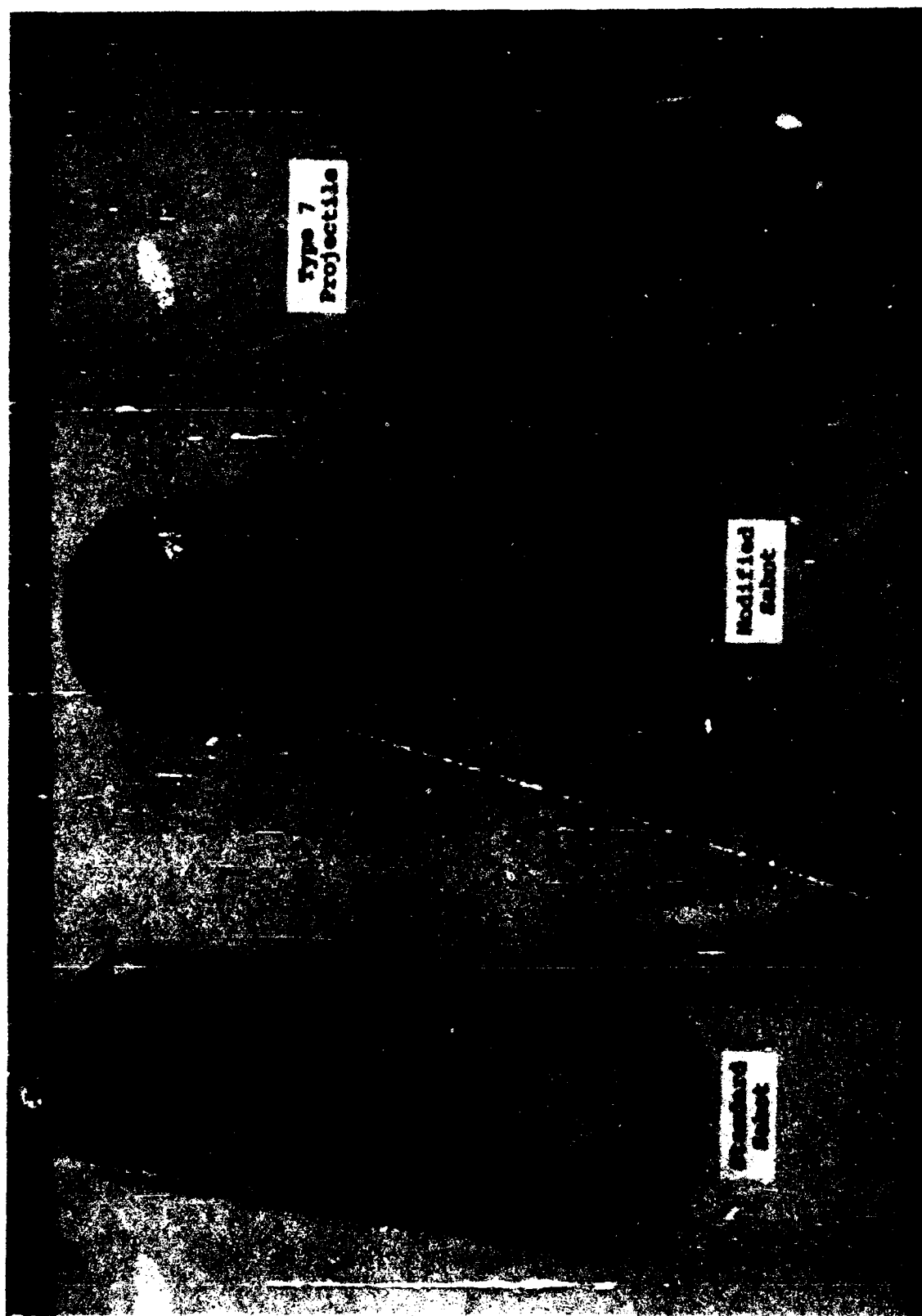


Figure 2.10. Typical Sabot Before and After Modification.

TABLE 2.1

AIR CANNON TEST MATRIX ARRANGED BY SPECIMEN GROUP

Specimen Group	Number of Specimens	PROJECTILE			Thickness ^a (in)	PLATE	
		Type	Diameter (in)	Mass (g)		Span (in)	Boundary Conditions ^b
A	4	1	1.0	67	.5	10 ^c	SS
B	4	1	1.0	67	.5	10 ^c	C
C	7	1	1.0	67	.5	4	C
D	7	1	1.0	67	.5	5	C
E	7	1	1.0	67	.5	8	C
F	7	1	1.0	67	.125	4	C
G	7	1	1.0	67	.25	4	C
H	7	2	.25	67	.5	5	C
I	7	3	.5	67	.5	5	C
J	7	4	1.5	67	.5	5	C
K	7	5	1.0	126	.5	5	C
L	4	6	1.0	290	.5	5	C
M	7	7	1.0	402	.5	5	C
N	4	1	1.0	67	.5	5	SS
O	7	1	1.0	67	.75	8	C
P	7	3	.5	67	.125	4	C
Q	7	2	.25	67	.125	4	C
R	7	5	1.0	126	.5	10 ^c	C
S	7	6	1.0	290	.5	10 ^c	C
T	7	7	1.0	403	.5	10 ^c	C
U	7	5	1.0	126	.5	8	C
V	7	6	1.0	290	.5	8	C
W	7	7	1.0	403	.5	8	C

^a Nominal thicknesses given. See text for actual thicknesses.

^b SS=Simply Support, C=Clamped

^c 10 in. x 10 in.-square opening; all others circular of given diameter.

TABLE 2.2

AIR CANNON TEST MATRIX ARRANGED BY TEST VARIABLE

Variable Investigated	Specimen Groups	PROJECTILE			PLATE		
		Type	diameter (in)	Mass (g)	Thickness ^a (in)	Span (in)	Boundary Conditions ^b
Boundary Conditions	A	1	1.	67	.5	10 ^c	SS
	B	1	1.	67	.5	10 ^c	C
	N	1	1.	67	.5	5	SS
	D	1	1.	67	.5	5	C
Plate Span	C	1	1.	67	.5	4	C
	D	1	1.	67	.5	5	C
	E	1	1.	67	.5	8	C
	B	1	1.	67	.5	10 ^c	C
Plate Thickness	F	1	1.	67	.125	4	C
	G	1	1.	67	.25	4	C
	C	1	1.	67	.5	4	C
	F	1	1.	67	.125	4	C
	G	1	1.	67	.25	4	C
	D	1	1.	67	.5	5	C
	O	1	1.	67	.75	8	C
Projectile Diameter	H	2	.25	67	.5	5	C
	I	3	.5	67	.5	5	C
	D	1	1.	67	.5	5	C
	J	4	1.5	67	.5	5	C
	Q	2	.25	67	.125	4	C
	P	3	.5	67	.125	4	C
	F	1	1.	67	.125	4	C
Projectile Mass and Velocity	D	1	1.	67	.5	5	C
	K	5	1.	126	.5	5	C
	L	6	1.	290	.5	5	C
	M	7	1.	402	.5	5	C
	B	1	1.	67	.5	10 ^c	C
	R	5	1.	126	.5	10 ^c	C
	S	6	1.	290	.5	10 ^c	C
	T	7	1.	403	.5	10 ^c	C
	E	1	1.	67	.5	8	C
	U	5	1.	126	.5	8	C
	V	6	1.	290	.5	8	C
	W	7	1.	403	.5	8	C

^a Nominal thicknesses given. See text for actual thicknesses.

^b SS = Simply Supported, C = clamped

^c 10 in. x 10 in.-square opening; all others circular of given diameter.

The results recorded for each test were specimen failure mode, absorbed energy to failure, and percent reduction in specimen thickness. To obtain specimen failure mode, the impact site of the tested specimens was observed, noting whether the specimen tended to fail in bending, shear, or tension.

Failure energy was defined as the minimum energy absorbed by the specimen that produced a visible, open crack, (see Figure 2.11). The failure energy was taken to be equal to the kinetic energy of the projectile (that is, all the projectile kinetic energy was assumed to be absorbed by the plate). The failure energy was therefore computed from

$$E = mv^2/2$$

where

$$\begin{aligned} E &= \text{failure energy, ft-lb} \\ M &= \text{projectile mass, lb-sec}^2/\text{ft} \\ V &= \text{projectile velocity, ft/sec} \end{aligned}$$

The seven replicates per test group allowed the projectile velocity to be varied on each shot so as to bracket and approach the failure energy.

Strain rates were recorded for comparison with those typical of birdstrike (see Section 1.1). Appendix A details the computation of these strain rates based on measured values of strain and projectile velocity. The computed values are time-averaged values of strain rates rather than instantaneous values; that is, they represent the average strain rate over the impact event duration rather than the strain rate at one specific instant of time.

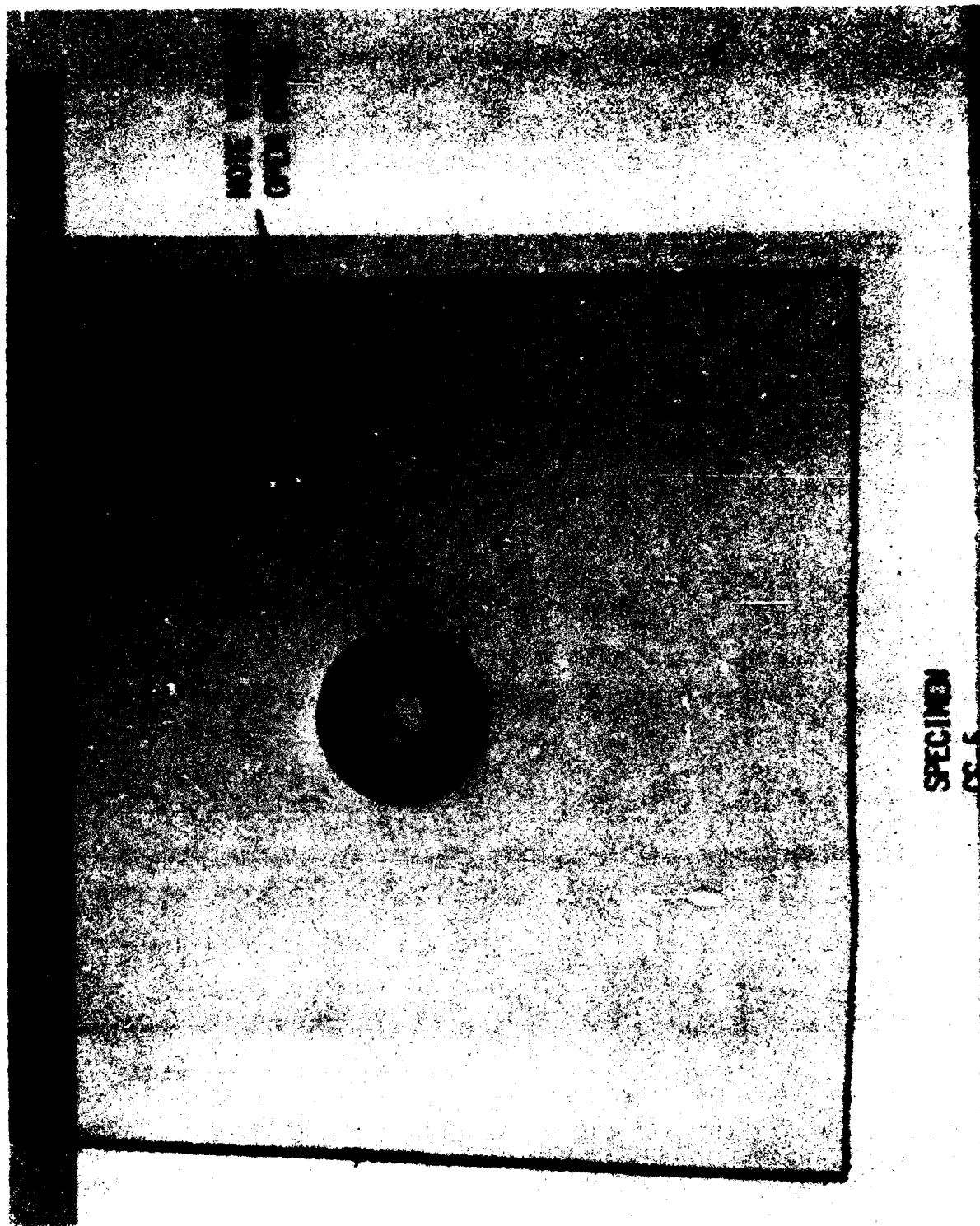


Figure 2.11. Typical Threshold of Failure Crack.

Percent reduction in specimen thickness was recorded to provide a measure of ductility. It was computed from

$$\% R = \frac{t - t_o}{t_o} \times 100\%$$

where

% R = percent reduction in thickness

t_o = specimen thickness before impact, inches

t = specimen thickness after impact, inches

Measurement of post-test thickness was performed with a micrometer generally at the center of impact.

2.4 FALLING WEIGHT TEST SETUP

The falling weight test setup is shown in Figure 2.12. The test apparatus consisted of a supporting frame and concrete base, adjustable span plate supports, clamping rings for fixing the specimen edges, loading noses, detachable, interchangeable, and variable-mass drop weights, two-cable system to guide the weights to specimen center at a velocity approaching free fall, automatic release mechanism, and rebound catch mechanism to prevent multiple impacts on a specimen due to impactor rebound.

Loading noses of AISI O1 steel were turned on a lathe to diameters of 0.25, 0.5 and 1.0 inches. They were hardened to Rc 47-50. The as-machined surface finish was approximately 80 μ in.

2.5 FALLING WEIGHT TEST PROCEDURE

Table 2.3 presents the falling weight test matrix. Nine sets of seven tests each were performed, for a total of 63 tests. The effects of plate span, plate thickness, and projectile

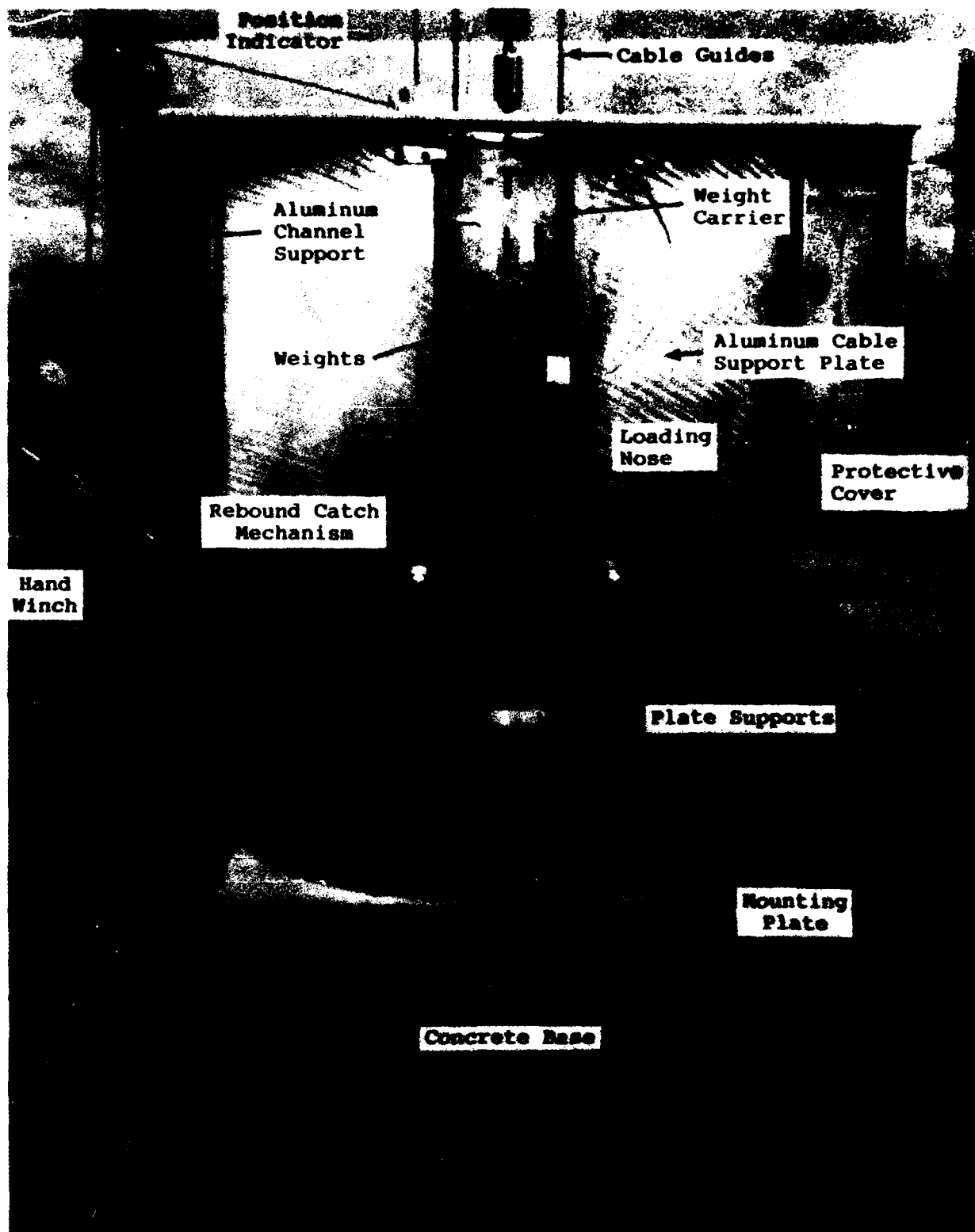


Figure 2.12. Falling Weight Test Apparatus for Plate Specimens.

TABLE 2.3
FALLING WEIGHT TEST MATRIX ARRANGED BY SPECIMEN GROUP

Specimen Group	Number of Specimens	Projectile Diameter (in)	Plate Thickness ^a (in)	Plate Span (in)	Plate Boundary Conditions ^b
FA	7	1.0	.5	8	C
FB	7	1.0	.5	4	C
FC	7	1.0	.125	4	C
FD	7	.5	.5	5	C
FE	7	.25	.5	5	C
FF	7	1.5	.5	5	C
FG	7	.25	.125	4	C
FH	7	.5	.125	4	C
FI	7	1.5	.125	4	C
DB ^c	15	1.0	.25	4	C
CC ^c	15	1.0	.5	5	C
DA ^{c,d}	13	1.0	.31	4	C

^aNominal thicknesses given. See text for actual thicknesses.

^bC = Clamped

^cTest results from Reference 2.

^dUncoated MIL-P-83310 polycarbonate.

diameter were investigated. Table 2.4 is a re-arrangement of Table 2.3 showing the test sets used to investigate each test parameter. Included are sets tested under a previous program² which were appropriate for this investigation and therefore not necessary to duplicate.

As with the air cannon tests, failure mode, absorbed energy, and percent thickness reduction were recorded (see Section 2.3). Failure energy was again defined as the minimum energy absorbed by the specimen that produced a visible, open crack. It was again assumed that, at failure, all of the projectile kinetic energy was absorbed by the plate. But the projectile kinetic energy at impact was (neglecting cable friction or air drag effects) equal to the projectile potential energy prior to release. Thus the failure energy for the plate was computed from

$$E = Wh$$

where

E = failure energy, ft-lbs

W = impactor weight, lbs

h = height of impactor above plate, ft

For each of the seven replicates within a test set the impactor weight and/or height were varied so as to bracket and approach the failure energy.

The methods for determining failure mode and percent thickness reduction were the same as those used for the air cannon tests.

TABLE 2.4
FALLING WEIGHT TEST MATRIX ARRANGED BY TEST VARIABLE

Variable Investigated	Specimen Groups	Projectile Diameter (in)	Plate Thickness ^a (in)	Plate Span (in)	Plate Boundary Conditions ^b
Plate Span	FB ^c	1.0	.5	4	C
	CC ^c	1.0	.5	5	C
	FA	1.0	.5	8	C
Plate Thickness	FC ^c	1.0	.125	4	C
	DB ^c	1.0	.25	4	C
	DA ^{c,d}	1.0	.31	4	C
	FB	1.0	.5	4	C
Projectile Diameter	FE	.25	.5	5	C
	FD ^c	.5	.5	5	C
	CC ^c	1.0	.5	5	C
	FF	1.5	.5	5	C
	FG	.25	.125	4	C
	FH	.5	.125	4	C
	FC	1.0	.125	4	C
	FI	1.5	.125	4	C

^aNominal thicknesses given. See text for actual thicknesses.

^bC = Clamped.

^cTest results from Reference 2.

^dUncoated MIL-P-83310 polycarbonate.

SECTION 3

RESULTS

3.1 AIR CANNON TEST RESULTS

A total of 158 air cannon tests were conducted. Table 3.1 summarizes the test results (i.e., strain rate, failure energy, failure mode, and percent thickness reduction) by specimen group. Table 3.2 summarizes the test results by the variable being investigated. Appendix B presents detailed test results for each specimen tested.

3.2 FALLING WEIGHT TEST RESULTS

A total of 56 falling weight tests were conducted. Table 3.3 summarizes the falling weight test results, including results of interest obtained from previous test programs. Table 3.4 summarizes the results by the variable being investigated. Appendix C presents detailed test results for each specimen tested.

3.3 DISCUSSION AND COMPARISON OF RESULTS

3.3.1 Strain Rates

In-plane, tension surface strains are reported in Tables 3.1-3.4 for all specimen groups except DA and DB. (Insufficient data was available for these groups since they were tested in a previous program.²) As mentioned in the Introduction, limited UDRI test data showed peak strain rates during room temperature birdstrike testing to be in the range of 100-450 in/in/sec, while Reference 3 cites strain rates of 30-200 in/in/sec.

Tables 3.3 and 3.4 indicate that the strain rates achieved by the falling weight tests were generally lower than

TABLE 3.1
AIR CANNON TEST RESULTS
SUMMARIZED BY SPECIMEN GROUP

Specimen Group	P R O J E C T I L E				P L A T E			Failure		Failure Mode	
	Type	Diameter (in)	Mass (g)	Velocity (ft/s)	Thickness (in)	Span (in)	Boundary Conditions ^b	Strain Rate (in/in/sec)	Energy (ft-lb)		Percent Thickness Reduction
A	1	1.0	67	851	.5	10 ^d	SS	890	1655	36	B
B	1	1.0	67	835	.5	10 ^d	C	1105	1595	42	B
C	1	1.0	67	731	.5	4	C	1334	1220	47	B
D	1	1.0	67	781	.5	5	C	1559	1395	42	B
E	1	1.0	67	795	.5	8	C	1253	1445	41	B
F	1	1.0	67	288	.125	4	C	1036	190	63	T
G	1	1.0	67	412	.25	4	C	873	390	54	B
H	2	.25	67	200	.5	5	C	358	93	54	B
I	3	.5	67	441	.5	5	C	605	445	52	B
J	4	1.5	67	961	.5	5	C	3003	2110	53	B
K	5	1.0	126	531	.5	5	C	793	1220	58	B
L	6	1.0	290	321	.5	5	C	413	1020	48	B
M	7	1.0	402	260	.5	5	C	404	930	59	B
N	1	1.0	67	803	.5	5	SS	1258	1470	31	B
O	1	1.0	67	1008	.75	8	C	865	2320	36	B
P	3	.5	67	165	.125	4	C	518	63	63	B
Q	2	.25	67	94	.125	4	C	310	20	61	B
R	5	1.0	126	645	.5	10 ^d	C	596	1800	51	B
S	6	1.0	290	422	.5	10 ^d	C	413	1765	52	B
T	7	1.0	403	335	.5	10 ^d	C	302	1545	59	B
U	5	1.0	126	613	.5	8	C	788	1620	49	B
V	6	1.0	290	412	.5	8	C	514	1685	56	B
W	7	1.0	403	307	.5	8	C	334	1300	52	B

- a Nominal Thicknesses given. See text for actual thicknesses.
b SS = simply supported, C = clamped.
c B = Bending (petalling), T = Tensile (cupping). (See Figures 3.8, 3.9)
d 10 in. x 10 in. square opening; all others circular of given diameter.

TABLE 3.2
AIR CANNON TEST RESULTS SUMMARIZED BY TEST VARIABLE

Variable Investigated	Specimen Groups	Type	P R O J E C T I L E			P L A T E			Strain Rate (in/in/sec)	Failure Energy (ft-lb)	Percent Thickness Reduction	Failure Mode
			Diameter (in)	Mass (g)	Velocity (ft/s)	Thickness ^a (in)	Span (in)	Boundary Conditions ^b				
Boundary Conditions	A	1	1.	67	851	.5	10 ^c	SS	890	1655	36	B
	B	1	1.	67	835	.5	10 ^c	C	1105	1595	42	B
	N	1	1.	67	803	.5	5	SS	1258	1470	31	B
	D	1	1.	67	781	.5	5	C	1559	1395	42	B
Plate Span	C	1	1.	67	731	.5	4	C	1334	1220	47	B
	D	1	1.	67	781	.5	5	C	1559	1395	42	B
	E	1	1.	67	795	.5	8	C	1253	1445	41	B
	B	1	1.	67	835	.5	10 ^c	C	1105	1595	42	B
Plate Thickness	F	1	1.	67	288	.125	4	C	1036	190	63	T
	G	1	1.	67	412	.25	4	C	873	390	54	B
	C	1	1.	67	731	.5	4	C	1334	1220	47	B
	F	1	1.	67	288	.125	4	C	1036	190	63	T
Projectile Diameter	G	1	1.	67	412	.25	4	C	873	390	54	B
	D	1	1.	67	781	.5	5	C	1559	1395	42	B
	O	1	1.	67	1008	.75	8	C	865	2320	36	B
	H	2	.25	67	200	.5	5	C	358	93	54	B
Projectile Mass and Velocity	I	3	.5	67	441	.5	5	C	605	445	52	B
	D	1	1.	67	781	.5	5	C	1559	1395	42	B
	J	4	1.5	67	961	.5	5	C	3003	2110	53	B
	Q	2	.25	67	94	.125	4	C	310	20	61	B
Projectile Mass and Velocity	P	3	.5	67	165	.125	4	C	518	63	63	B
	F	1	1.	67	288	.125	4	C	1036	190	63	T
	D	1	1.	67	781	.5	5	C	1559	1395	42	B
	K	5	1.	126	531	.5	5	C	793	1220	58	B
Projectile Mass and Velocity	L	6	1.	290	321	.5	5	C	413	1020	48	B
	M	7	1.	402	260	.5	5	C	404	930	59	B
	B	1	1.	67	835	.5	10 ^c	C	1105	1595	41	B
	R	5	1.	126	645	.5	10 ^c	C	596	1800	51	B
Projectile Mass and Velocity	S	6	1.	290	422	.5	10 ^c	C	413	1765	52	B
	T	7	1.	403	335	.5	10 ^c	C	302	1545	59	B
	E	1	1.	67	795	.5	8	C	1253	1445	41	B
	U	5	1.	126	613	.5	8	C	788	1620	49	B
Projectile Mass and Velocity	V	6	1.	290	412	.5	8	C	514	1685	56	B
	W	7	1.	403	307	.5	8	C	334	1300	52	B

^aNominal thicknesses given. See text for actual thicknesses.

^bSS = Simply Supported; C = Clamped.

^c10 in. x 10 in. square opening; all others circular of given diameter.

^dB = Bending (petalling), T = Tensile (cupping) (See Figures 3.8, 3.9)

TABLE 3.3
FALLING WEIGHT TEST RESULTS
SUMMARIZED BY TEST GROUP

Specimen Group	P R O J E C T I L E			P L A T E		Failure Energy (ft-lb)	Percent Thickness Reduction	Failure Mode ^c
	Diameter (in)	Mass (lb)	Velocity (ft/s)	Thickness ^a (in)	Span (in)	Boundary Conditions ^b	Strain Rate (in/in/sec)	
FA	1.0	60.57	31.1	.5	8	C	39	912 56 B
FB	1.0	55.0	31.7	.5	4	C	49	860 57 B
FC	1.0	14.03	28.4	.125	4	C	98	176 54 T
FD	.5	24.45	28.1	.5	5	C	41	300 56 B
FE	.25	6.89	27.9	.5	5	C	51	83 32 S
FF	1.5	-----	-----	.5	5	C	-----	-----
FG	.25	2.2	23.6	.125	4	C	98	19 60 B
FH	.5	5.24	26.0	.125	4	C	104	55 63 TB
FI	1.5	23.4	28.6	.125	4	C	50	298 46 T
DB	1.0	33.0	27.2	.25	4	C	e	380 60 B
CC	1.0	48.0	34.1	.5	5	C	49	865 65 B
DA	1.0	28.5	32.8	.31	4	C	e	475 59 B

^aNominal thicknesses given. See text for actual thicknesses.

^bC = Clamped.

^cB = Bending (petalling), T = Tensile (cupping), S = Shear (plugging). (See Figures 3.8, 3.9, 3.10)

^dSpecimens not tested because needed failure energy could not be achieved (drop height and weight were limited).

^eInsufficient data available from previous test program from which to compute strain rate.

TABLE 3.4
FALLING WEIGHT TEST RESULTS
SUMMARIZED BY TEST VARIABLE

Variable Investigated	Specimen Groups	P R O J E C T I L E			P L A T E			Failure Energy (ft-lb)	Percent Thickness Reduction	Failure Mode ^c
		Diameter (in)	Mass (lb)	Velocity (ft/s)	Thickness ^a (in)	Span (in)	Boundary Conditions ^b			
Plate	FB	1.0	55.0	31.7	.5	4	C	860	57	B
Span	CC	1.0	48.0	34.1	.5	5	C	865	65	B
	FA	1.0	60.57	31.1	.5	8	C	912	56	B
Plate	FC	1.0	14.03	28.4	.125	4	C	176	55	T
Thickness	DB	1.0	33.0	27.2	.25	4	C	380	60	B
	DA	1.0	28.5	32.8	.31	4	C	475	59	B
	FB	1.0	55.0	31.7	.5	4	C	865	57	B
Projectile	FG	.25	2.2	23.6	.125	4	C	19	60	B
Diameter	FH	.5	5.24	26.0	.125	4	C	55	63	TB
	FC	1.0	14.03	28.4	.125	4	C	176	55	T
	FI	1.5	23.40	28.6	.125	4	C	298	46	T
	FE	.25	6.89	27.9	.5	5	C	83	32	S
	FD	.5	24.45	28.1	.5	5	C	300	56	B
	CC	1.0	48.0	34.1	.5	5	C	865	65	B

^aNominal thicknesses given. See text for actual thicknesses.

^bC = Clamped.

^cB = Bending (petalling), T = Tensile (cupping), S = Shear (plugging). (See Figures 3.8, 3.9, 3.10)

^dInsufficient data available from previous test program from which to compute strain rate.

the range of typical birdstrike values (100-450 in/in/sec). However, strain rates of 90-100 in/in/sec were achieved for thin (0.125 in.) plates at small (4 in.) spans impacted by small-to-moderate diameter noses (0.25-1.0 in.).

Tables 3.1 and 3.2 report air cannon strain rates that are an order of magnitude larger than the falling weight values. Many of the air cannon strain rates lay within the range of typical birdstrike values, although the majority of air cannon values are outside (higher than) this range. Strain rates characteristic of birdstrike were achieved for both thick (0.5 in.) and thin (0.125 in.) plates. The data indicates that strain rates decrease (toward birdstrike values) with decreasing projectile diameter and decreasing projectile velocity (increasing projectile mass). In an air cannon polycarbonate screening program, it therefore appears that by varying these parameters, it is possible to achieve strain rates characteristic of birdstrike for arbitrary geometries (thickness, span, boundary condition) of polycarbonate specimens.

3.3.2 Failure Energy

Figures 3.1-3.3 present plots of failure energy versus plate span, plate thickness, and projectile diameter, respectively, for both air cannon and falling weight data. For each plot, all geometric parameters (plate span and thickness, impactor diameter, and boundary conditions) were identical for the air cannon and falling weight data except for the parameter being varied. Non-dimensionalizing of the plotted parameters was not practical because of plasticity, edge effects, and change in failure mode.

From Figures 3.1-3.3 it is apparent that failure energy increased with increasing plate thickness, plate span, and projectile diameter for both the falling weight and air cannon test results. The failure energies for the air cannon tests were

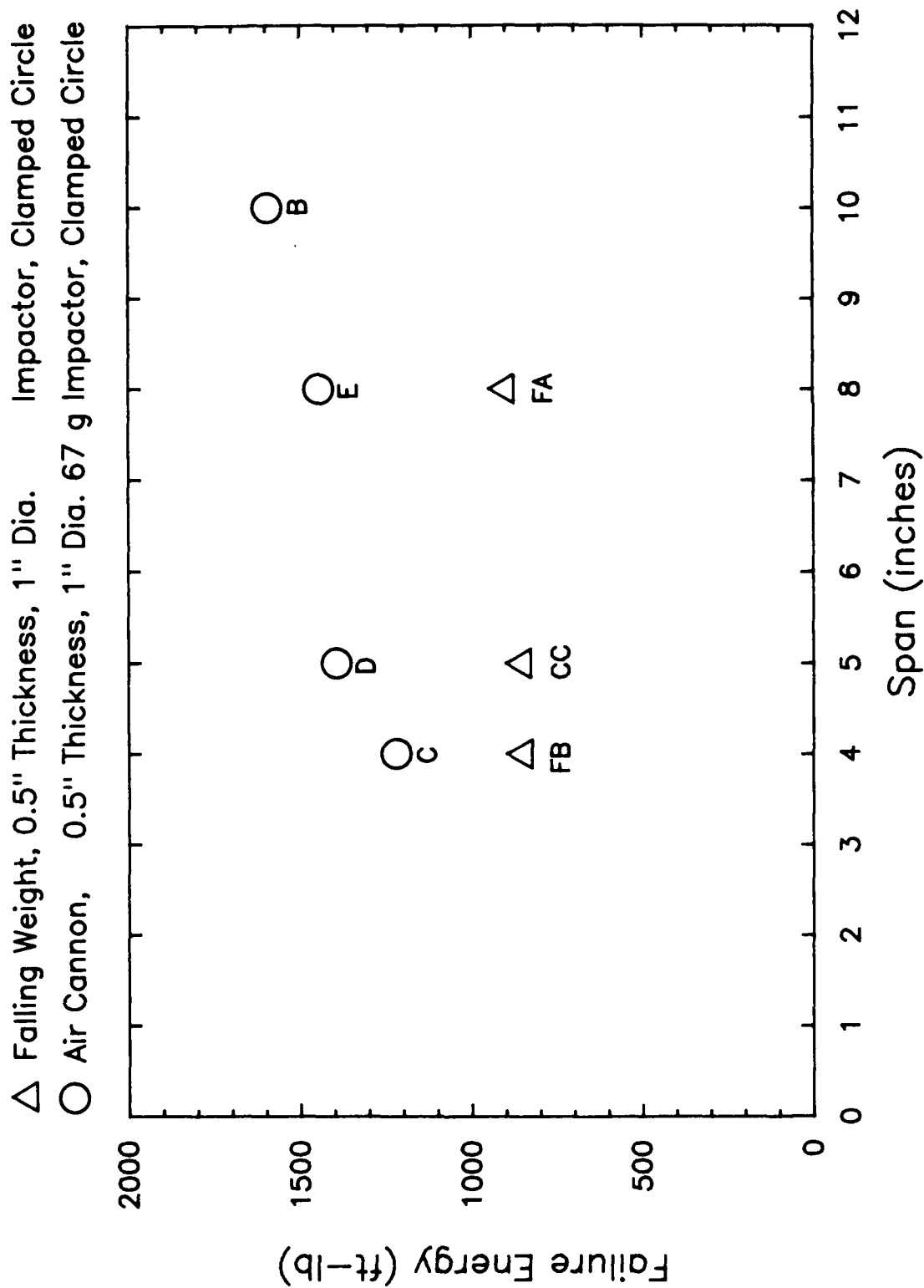


Figure 3.1. Comparison of Failure Energy versus Plate Span for Similar Air Cannon and Falling Weight Tests.

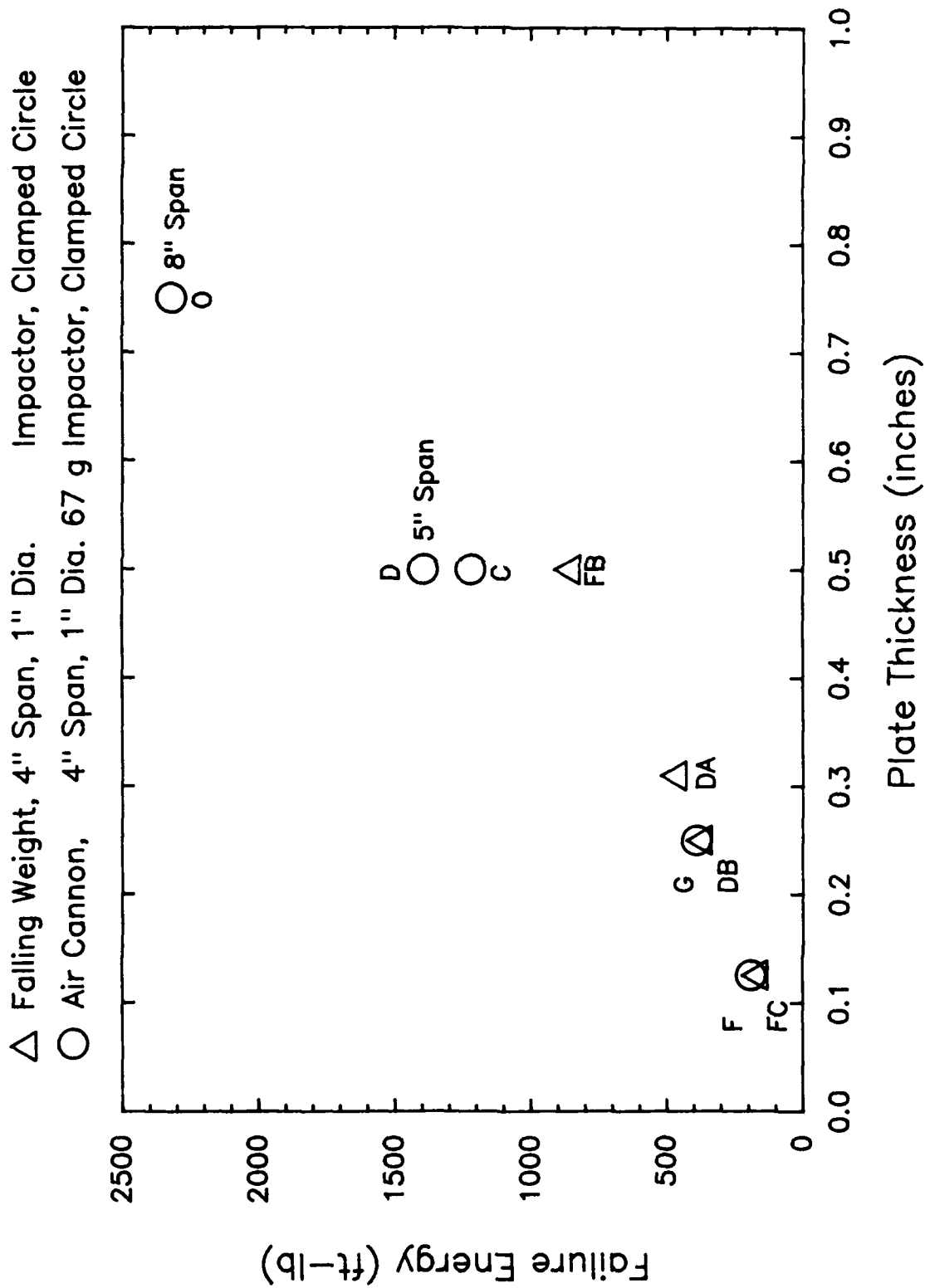


Figure 3.2. Comparison of Failure Energy versus Plate Thickness for Similar Air Cannon and Falling Weight Tests.

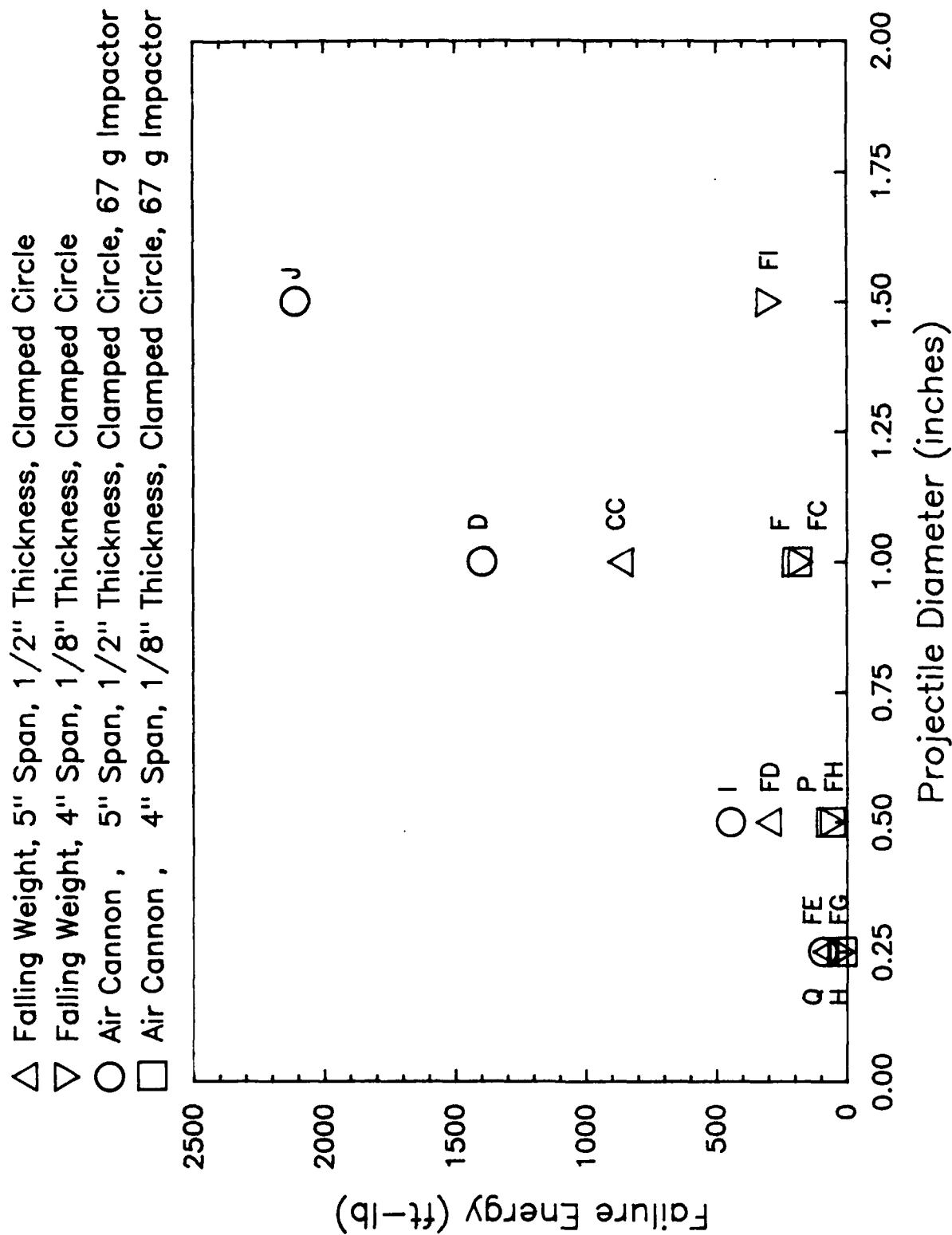


Figure 3.3. Comparison of Failure Energy versus Projectile Diameter for Similar Air Cannon and Falling Weight Tests.

greater than or equal to the failure energies for the falling weight tests, perhaps due to strain rate dependencies of the polycarbonate. The results indicate that the failure energies were nearly equal for thin ($1/8$ in.) specimens. As the thickness increased, however, the air cannon energies increase more rapidly than did the falling weight energies. (See Figures 3.1 and 3.3).

Figure 3.1 indicates that the failure energy shows a relatively small increase with increasing plate span, as compared with increasing plate thickness of Figure 3.2. Based on the tests conducted, it therefore appears that failure energy of the plates is controlled more strongly by plate thickness than plate span. This indicates that plate failure is primarily a local phenomena near the point of impact, where the thickness to be penetrated is the primary energy-controlling factor, as compared with overall bending failure, where span would become an important factor. These results coincide with the failure mode observations (Section 3.4) and with Reference 2.

Figure 3.3 indicates that the rate of increase of failure energy with increasing projectile diameter depended on specimen thickness. That is, the greater the thickness, the more sensitive was failure energy to projectile diameter (i.e., the steeper is the slope of the energy-diameter curve). For small thicknesses ($1/8$ in.) the failure energies for the air cannon and falling weight tests were similar. For greater thicknesses, the air cannon energies were greater than those for the falling weight tests. For small projectile diameters ($1/4$ in.) there was little difference in failure energy between air cannon and falling weight data, regardless of plate thickness. As projectile diameter increased the air cannon failure energy increased more rapidly than the falling weight failure energy for thick (0.5 in.) plates.

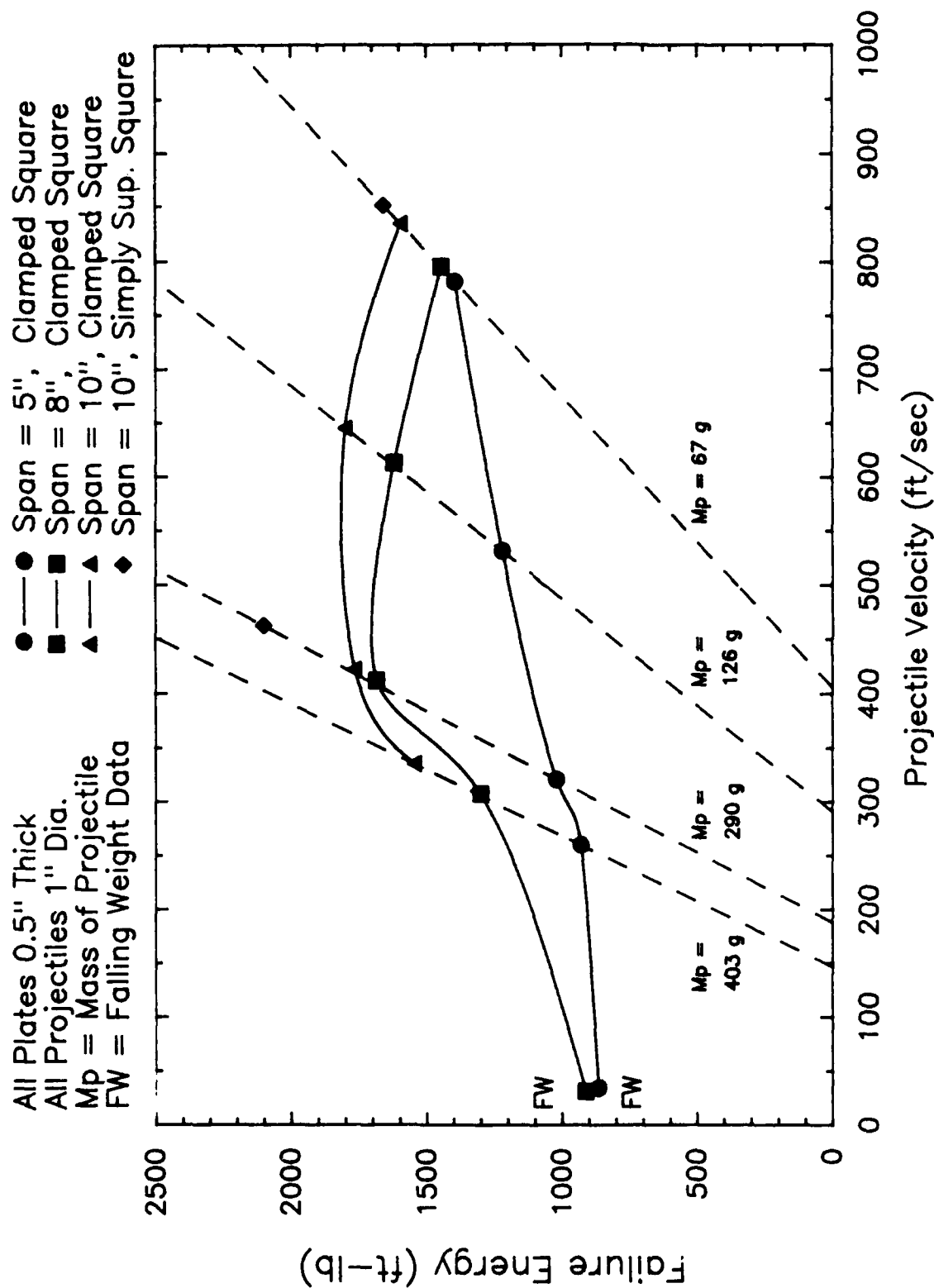


Figure 3.4. Variation of Failure Energy with Projectile Velocity for Various Plate Spans (air cannon tests except as noted).

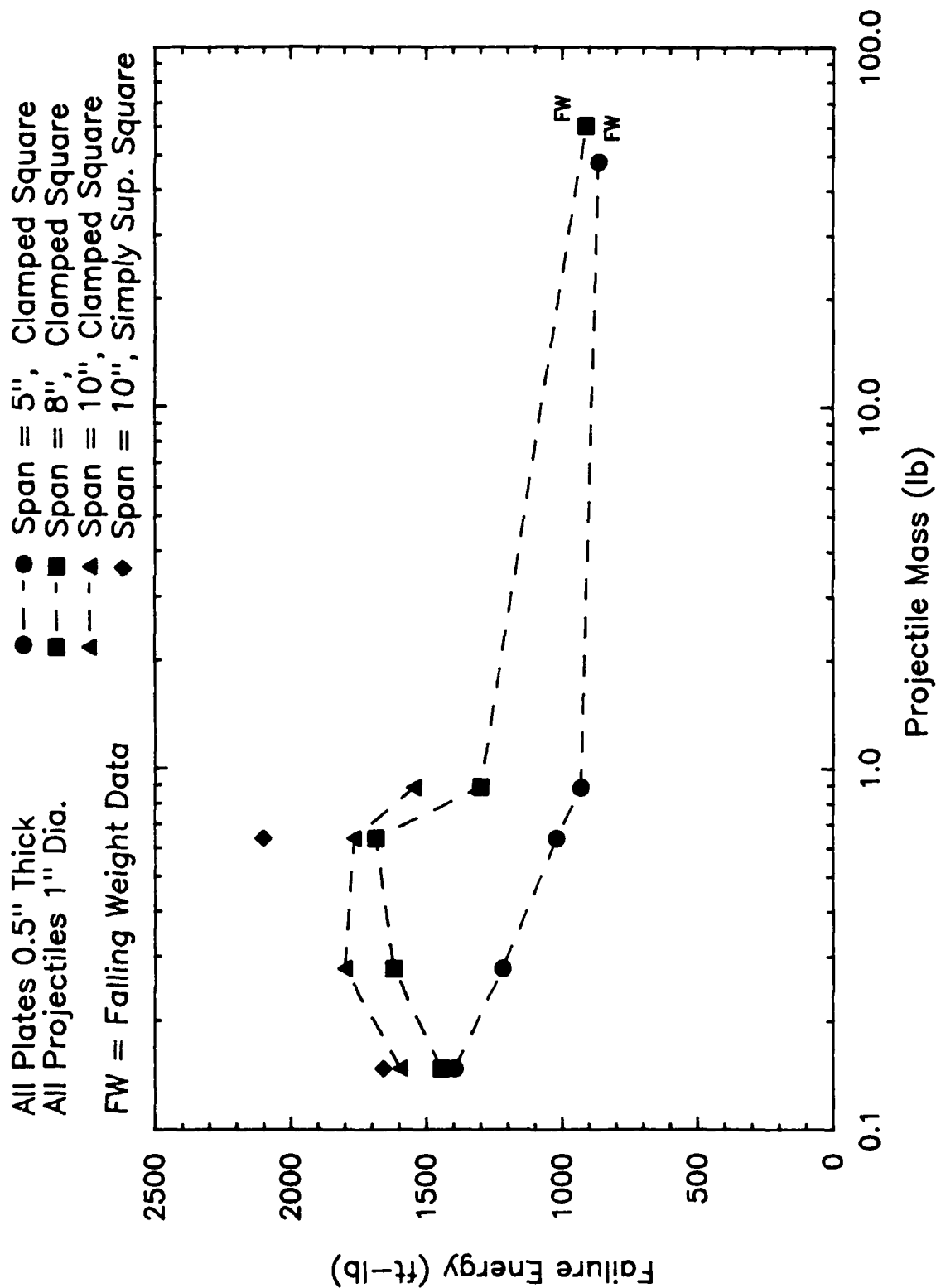


Figure 3.5. Variation of Failure Energy with Projectile Mass for Various Plate Spans (air cannon tests except as noted).

In Reference 2 it was noted that, for the few tests conducted, the air cannon failure energy varied with projectile velocity. Additional tests were performed as part of the present study to verify this finding. Figures 3.4 and 3.5 present the results.

Figure 3.4 shows plots of energy versus projectile velocity for 0.5-inch-thick plates and 1.0-inch diameter impactors for various plate spans. Included in the plot are falling weight results, which represent low velocity impacts, and the results from Reference 2. The various velocities were obtained by varying the projectile mass. Increasing mass led to decreasing velocity at failure and conversely.

The plot indicates that for the relatively thick (0.5 inch) specimens the failure energy changed with velocity. For the 5-inch span results, the energy increased continually and non-linearly with velocity. For the 8-inch and 10-inch span results the energy increased non-linearly with increasing velocity to a peak value, after which it decreased non-linearly with increasing velocity. There was apparently a transition span below which the energy increased monotonically and above which it exhibited a peak value. The non-linearities of the energy versus velocity curves may have been due to strain rate dependent stiffening of the polycarbonate, specimen inertia (energy is required to accelerate the portions of the specimen being deformed; the significance may decrease as velocity increases because deformation becomes more localized), and vibration effects (overall plate bending modes and elastic wave propagation).

It was previously stated that, based on Figure 3.1, failure energy depended only mildly on plate span. The air cannon tests done for the span evaluation were performed with a 67-gram spherical projectile, resulting in the highest range of

failure velocities of any of the impactors used. Figure 3.4 shows that the failure energies for the 67g impacts did not vary greatly with changing plate span. But Figure 3.4 also indicates that for heavier impactors, resulting in lower failure velocities, changing plate span resulted in a large change in failure energy. Thus the effect of plate span on failure energy depended on the projectile mass, and therefore projectile velocity. The observations noted previously in this section concerning the effects of plate thickness and projectile diameter on failure energy may also be velocity dependent. No data was gathered to test these dependencies.

It is informative to observe the low and high velocity extremes of Figure 3.4. At falling weight test velocities (below 50 ft/sec) the energy-velocity curves tend to flatten out. Thus for any change in velocity the change in failure energy is insignificant. This effect is also shown in the energy versus projectile mass plots of Figure 3.5. In other words, the failure energies for falling weight tests are not velocity dependent. In addition, the effect of plate span on failure energy does not depend on projectile velocity for falling weight tests.

At the highest air cannon velocities it appears that the failure energies for the different spans are converging to a single value. This would indicate that plate span has a decreasing influence on failure energy as velocity becomes large. This means that plate failure becomes highly localized at high velocities. The various curves of Figure 3.4 would therefore be expected to level out to a single energy value at very high velocities. More test data with light-weight (30 grams or less) projectiles would be needed to verify this hypothesis.

In summary, for the tests performed, the air cannon and falling weight failure energies showed similar trends.

That is, failure energy increased with increasing plate span, plate thickness, and projectile diameter, and decreasing edge fixity. Plate thickness appeared to have the greatest effect on failure energy of the three geometric parameters (that is, doubling the thickness changed failure energy more than doubling span or projectile diameter).

The air cannon failure energies were consistently greater than or equal to the falling weight failure energies. The strain-rate dependent behavior of the polycarbonate may have contributed to the difference in failure energies. For thin (1/8 inch) plates and small (1/4 inch) diameter projectiles, however, the difference was negligible.

For the falling weight tests the failure energies were found to be independent of impactor mass/velocity, so that the energy versus parameter trends and dependencies were predictable. The air cannon results, however, were found to be strongly velocity dependent in non-linear fashion. The energy versus parameter trends and dependencies reported in this section may therefore change for other combinations of projectile mass/velocity. Using the air cannon test method for material screening would require accurately knowing the velocity dependencies of the test parameter. More testing is needed to fully characterize these velocity dependencies.

3.3.3 Failure Mode

In Section 2.3 threshold of failure was defined as a visible, open crack in the material due to projectile impact. In practice, visible, open cracking was achieved fairly regularly with the falling weight test method but very seldom with the air cannon test method. Air cannon specimens either plastically deformed without cracking or allowed penetration of the projectile. One phenomena that was achieved fairly regularly and which may provide a more practical alternative to the threshold

of failure in air cannon testing was the ballistic limit.^{5,6} The ballistic limit is defined here as minimum penetration of the specimen, that is, the projectile penetrates the specimen and either imbeds itself in it (see Figure 3.6) or exits the specimen with nearly zero velocity, so that it drops to the ground. For a given test setup, the ballistic limit energy would be higher than the threshold of failure energy though it is felt that the difference would be small, because much more energy would be required to form a crack than to open an existing one. Additional testing would be needed to verify this hypothesis.

Overall plastic bending of the plates was investigated. The amount of overall deformation depended on the velocity of impact. Lower velocities resulted in more deformation because the entire plate had more time to bend before failure, whereas high velocities caused local failure before much overall bending occurred. Thus, falling weight test specimens showed more overall permanent deformation than did the air cannon specimens (see Figure 3.7). The same trend was observed among air cannon test specimens impacted at different velocities, although the amount of permanent deformation for any of the velocities was small compared with the falling weight test specimens. The overall bending of the falling weight specimens may have provided a significant component of stress in the tension surface that was small for the air cannon specimens, contributing in part to the lower failure energies noted in Section 3.1.

Observation of failed (penetrated) plate failure modes were made. Three distinct failure modes were noted. The most common was "petalling", a local bending failure whereby the material reached its ultimate strength at the surface in tension, causing the specimen to split open into two or more lobes or petals (see Figure 3.8). The next most common failure was "cupping", a tensile failure whereby the material was ductilely

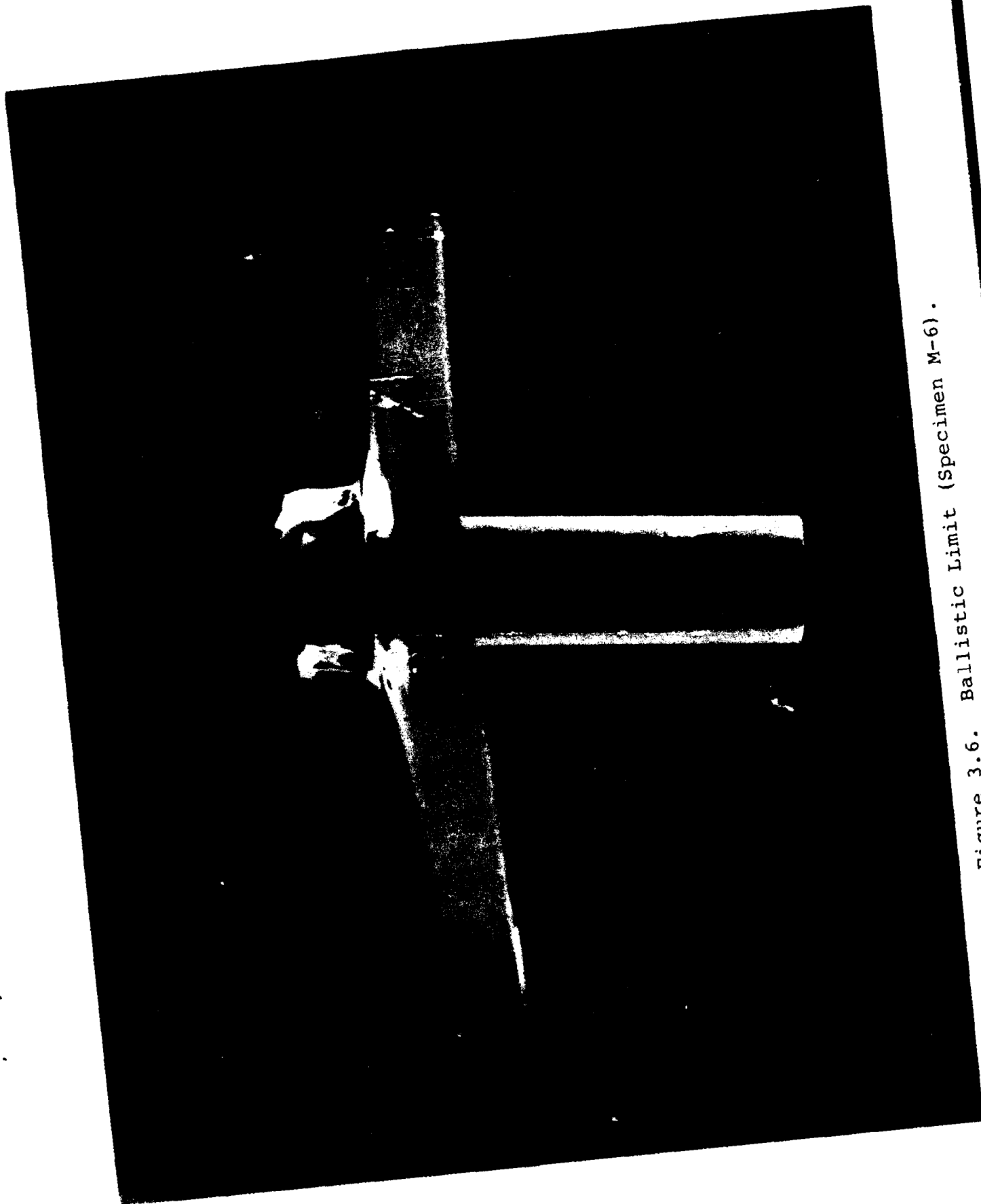


Figure 3.6. Ballistic Limit (Specimen M-6).



Figure 3.7. Comparison of Overall Plate Bending for Similar Air Cannon and Falling Weight Specimens.

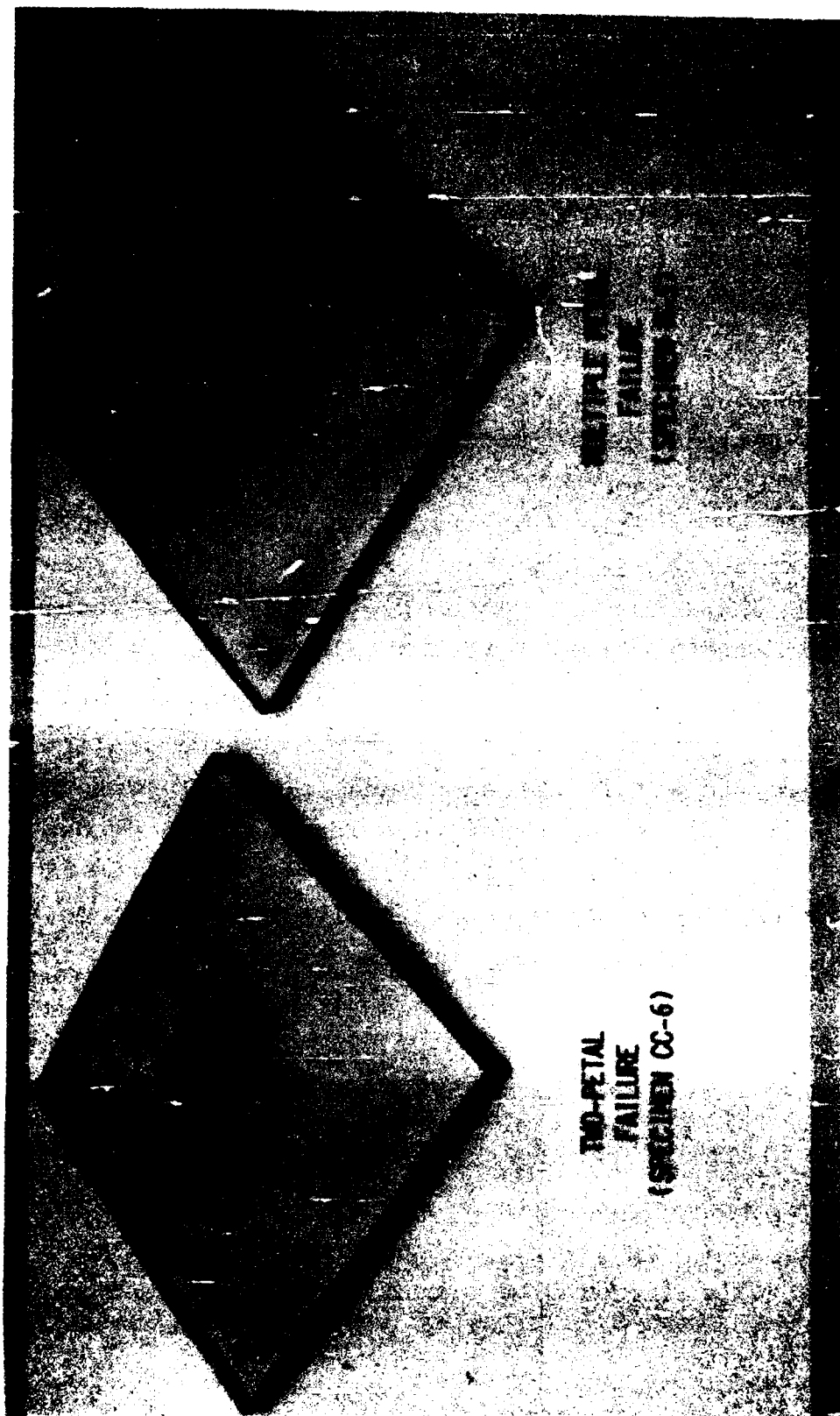


Figure 3.8. Typical Petalling (Bending) Failures.

stretched out by the projectile until large in-plane (tensile) loads developed, which exceeded the material's ultimate strength, causing a "cup" to be punched out around the nose of the impactor (see Figure 3.9). The third failure mode, termed "plugging", occurred only during one group of falling weight tests (group FE), and not during air cannon tests. Plugging was a shear failure of the specimen whereby a cylinder (plug) of material, of diameter equal to that of the projectile, was punched out of the specimen (see Figure 3.10). All of the failure modes observed are commonly noted in the ballistic penetration literature.^{5,7,8}

Table 3.5 summarizes the failure modes for similar air cannon and falling weight test setups. The failure modes for the two test methods were, with one exception, identical for a given specimen and projectile geometry. The only exception was for a narrow impactor (0.25-inch diameter) on a relatively thick plate (0.5 inch), where the air cannon plates failed by petalling while the falling weight plates failed by plugging.

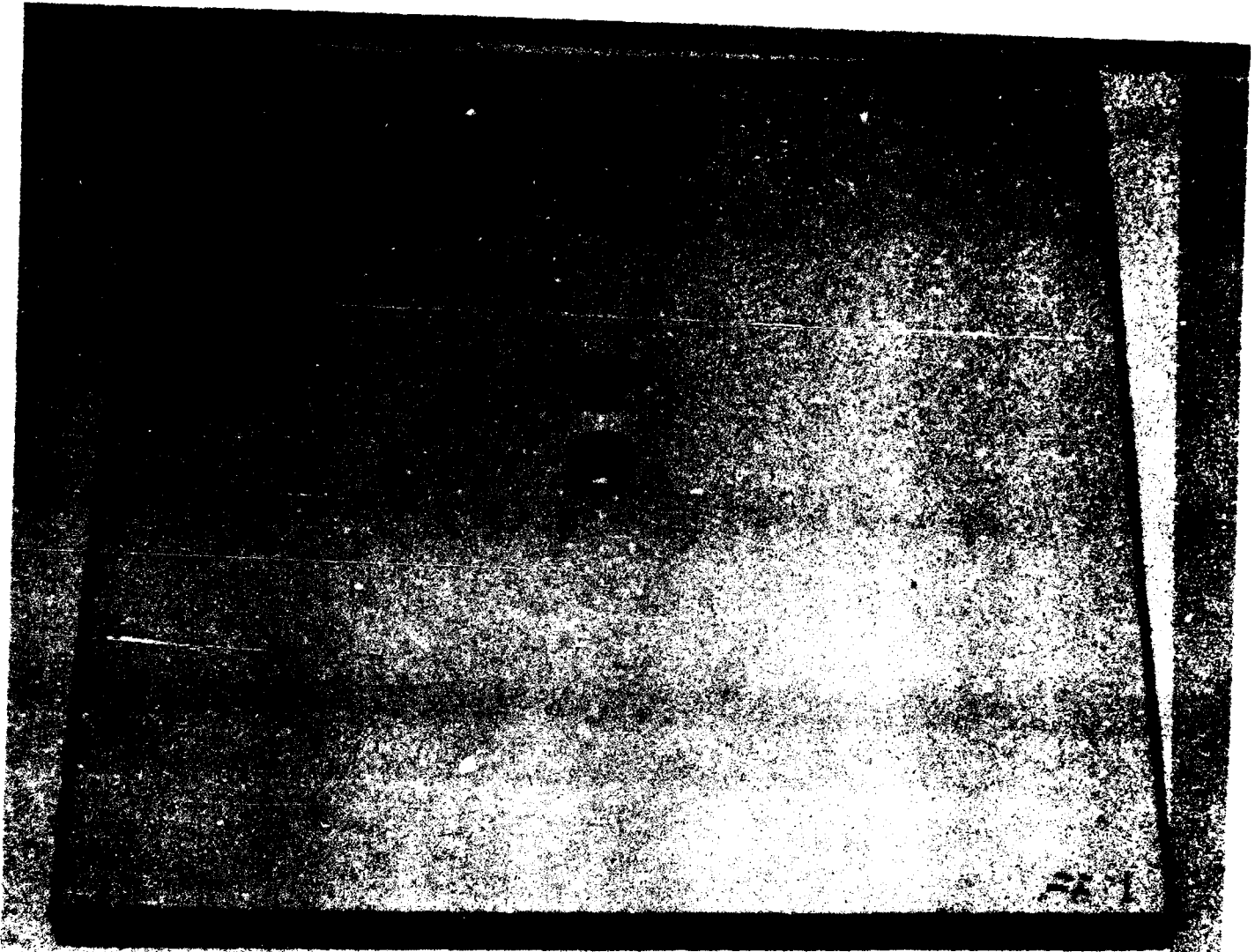
From Table 3.5 it appears that plate span had no influence on failure mode. Plate thickness and projectile diameter did, however, influence, and apparently determined, the failure mode. These two parameters were not independent, but interacted to determine the failure mode. The ratio of the two parameters appears to have determined the failure mode. The following correlation of diameter-to-thickness (d/t) and failure mode are drawn from Table 3.5:

$d/t < 1/2$	----->	Plugging
$1 \leq d/t \leq 4$	----->	Petalling
$d/t > 4$	----->	Cupping

These guidelines, with verification and refinement from additional testing, could be used to ensure a given failure mode



Figure 3.9. Typical Cupping (Tensile) Failure.



**SPECIMEN
FE-1**

Figure 3.10. Typical Plugging (Shear) Failure.

TABLE 3.5
COMPARISON OF AIR CANNON AND FALLING WEIGHT FAILURE MODES
VERSUS GEOMETRIC TEST VARIABLE

Geometric Test Variable	Projectile Diameter (in)	Plate Thickness ^a (in)	Plate Span (in)	Air Cannon		Falling Weight	
				Specimen Group	Failure Mode ^b	Specimen Group	Failure Mode ^b
Plate Span	1.0	.5	4	C	B	FB	B
	1.0	.5	5	D	B	CC	B
	1.0	.5	8	E	B	FA	B
	1.0	.5	10	B	B	--	-
Plate Thickness	1.0	.125	4	F	T	FC	T
	1.0	.25	4	G	B	DB	B
	1.0	.31	4	-	-	DA	B
	1.0	.5	4	C	B	FB	B
Projectile Diameter	.25	.5	5	H	B	FE	S
	.5	.5	5	I	B	FD	B
	1.0	.5	5	D	B	CC	B
	1.5	.5	5	J	B	--	-
	.25	.125	4	Q	B	FG	B
	.5	.125	4	P	B	FH	BT
	1.0	.125	4	F	T	FC	T

^aNominal thicknesses listed. See text for actual thicknesses.

^bB = Bending (petalling), T = Tensile (cupping), S = Shear (plugging).

is achieved in designing a material screening test program. Based on the data of Table 3.5, these guidelines appear to apply to both falling weight and air cannon test results, although, as previously mentioned, there was a difference in failure mode for $d/t = 1/2$.

The dependency of failure mode on projectile velocity was also investigated. Table 3.6 summarizes the failure modes for various impact velocities. The results indicate that velocity did not affect failure mode for the air cannon tests. It should be noted, however, that velocity probably had some influence on failure mode, based on comparison of air cannon and falling weight tests. Air cannon test group H failed in petalling while the corresponding falling weight test group FE failed in plugging. All test conditions were identical except for projectile mass and velocity. The difference in velocity therefore appears to have caused the difference in failure modes between these test groups.

In summary, the failure modes were generally the same for identical air cannon and falling weight test setups. Span did not influence failure mode of either test method. Velocity had little influence on failure mode, leading to differences between air cannon and falling weight results in only one test configuration. The ratio of projectile diameter to plate thickness was noted to correlate well with the three observed failure modes. Overall plastic bending of the plates increased with decreasing impact velocity. The stress induced by this deformation may have contributed to the lower falling weight failure energies (as compared with the corresponding air cannon energies). Finally, threshold of failure was difficult to achieve in practice with the air cannon test. The ballistic limit may provide a more practical failure initiation criteria for air cannon tests.

TABLE 3.6
COMPARISON OF AIR CANNON AND FALLING WEIGHT FAILURE MODES
VERSUS PROJECTILE VELOCITY

Specimen Group	Test Type ^a	P R O J E C T I L E			P L A T E			Failure Mode
		Diameter (in)	Mass (lb)	Velocity (ft/s)	Thickness ^b (in)	Span (in)	Strain Rate (in/in/sec)	
E	AC	1.	.15	835	.5	8	1240	B
U	AC	1.	.28	613	.5	8	956	B
V	AC	1.	.64	412	.5	8	643	B
W	AC	1.	.89	307	.5	8	479	B
FA	FW	1.	60.57	31.1	.5	8	49	B
D	AC	1.	.15	781	.5	5	2413	B
K	AC	1.	.28	531	.5	5	1641	B
L	AC	1.	.64	321	.5	5	992	B
M	AC	1.	.89	260	.5	5	803	B
CC	FW	1.	48.0	34.1	.5	5	105	B

^aAC = Air Cannon; FW = Falling Weight

^bNominal thicknesses listed. See text for actual thicknesses.

NOTE: All plate edges clamped.

3.3.4 Percent Reduction in Thickness

The post-test thickness was often found difficult to measure because of the jaggedness of the failed surfaces. This was especially true of the air cannon specimens. It was found that the greatest reduction in thickness generally occurred at the center of impact of the falling weight specimens and off-center (near the shoulder of the deformed region) for the air cannon specimens, indicating more shearing of the air cannon specimens.

Tables 3.7 and 3.8 summarize and compare percent reduction in thickness data for the air cannon and falling weight tests. The falling weight data showed no correlation with plate span, plate thickness, or impactor diameter. The air cannon results showed no correlation with plate span or projectile diameter. (Reference 2 indicated that percent reduction in thickness increased with decreasing projectile diameter.) However, the percent reduction in thickness did decrease with increasing plate thickness. From Table 3.8 it also appears that the percent reduction in thickness was velocity dependent. The percent reduction in thickness decreased with increasing velocity (decreasing mass). (Reference 2 did not show any velocity dependency but air cannon data was limited.) The falling weight test percent thickness reductions were thus generally greater than the air cannon results, so that the falling weight test provided greater sensitivity to percent reduction in thickness. The data in Table 3.7, when compared with failure mode data, shows that percent reduction in thickness changed little when transitioning from cupping to petalling failure, but did decrease sharply when transitioning from petalling to plugging.

In summary, Reference 2 concludes that percent reduction in thickness may provide a means of comparing impact resistances of polycarbonate specimens even if geometric parameters such as

TABLE 3.7
COMPARISON OF AIR CANNON AND FALLING WEIGHT PERCENT THICKNESS REDUCTION
VERSUS GEOMETRIC TEST VARIABLE

Geometric Test Variable	Projectile Diameter (in)	Plate Thickness ^a (in)	Plate Span (in)	Air Cannon		Falling Weight	
				Specimen Group	%Thickness Reduction	Specimen Group	%Thickness Reduction
Plate Span	1.0	.5	4	C	47	FB	57
	1.0	.5	5	D	42	CC	65
	1.0	.5	8	E	41	FA	56
	1.0	.5	10	B	42	--	--
Plate Thickness	1.0	.125	4	F	63	FC	54
	1.0	.25	4	G	54	DB	60
	1.0	.31	4	-	-	DA	59
	1.0	.5	4	C	47	FB	57
Projectile Diameter	.25	.5	5	H	54	FE	32
	.5	.5	5	I	52	FD	56
	1.0	.5	5	D	42	CC	65
	1.5	.5	5	J	53	--	--
	.25	.125	4	Q	61	FG	60
	.5	.125	4	P	63	FH	63
	1.0	.125	4	F	63	FC	65

^aNominal thicknesses listed. See text for actual thicknesses.

TABLE 3.8
COMPARISON OF AIR CANNON AND FALLING WEIGHT PERCENT THICKNESS REDUCTION
VERSUS PROJECTILE VELOCITY

Specimen Group	Test Type ^a	P R O J E C T I L E			P L A T E			Thickness Reduction
		Diameter (in)	Mass (lb)	Velocity (ft/s)	Thickness ^b (in)	Span (in)	Strain Rate (in/in/s)	
E	AC	1.	.15	835	.5	8	1240	41
U	AC	1.	.28	613	.5	8	956	49
V	AC	1.	.64	412	.5	8	643	56
W	AC	1.	.89	307	.5	8	479	52
FA	FW	1.	60.57	31.1	.5	8	49	56
D	AC	1.	.15	781	.5	5	2413	42
K	AC	1.	.28	531	.5	5	1641	58
L	AC	1.	.64	321	.5	5	992	48
M	AC	1.	.89	260	.5	5	803	59
CC	FW	1.	48.0	34.1	.5	5	105	65

$$^a_{AC} = \text{Air Cannon; FW} = \text{Falling Weight}$$

^bNominal thicknesses listed. See text for actual thicknesses.

NOTE: All plate edges clamped.

plate thickness differ between the specimens being compared. The data collected in the present study supports this conclusion with respect to falling weight testing. The falling weight data was independent of plate and projectile geometry and projectile velocity. The only dependency observed was with failure mode. Thus percent reduction in thickness is a very flexible means of comparing impact resistances of polycarbonate plates tested by the falling weight technique. The air cannon percent reduction in thickness depended on plate thickness and projectile velocity as well as failure mode. These dependencies limit the flexibility of the percent reduction in thickness in comparing impact resistances of various polycarbonate plate specimens tested by the air cannon technique.

SECTION 4

CONCLUSIONS

The following conclusions were reached as a result of this investigation.

1. The air cannon strain rates were generally higher than those typical of birdstrike. However, strain rates in the range typical of birdstrike were achieved for both thin (0.125 inch) and thick (0.5 inch) plates. The data indicates that it may be possible to achieve strain rates characteristic of birdstrike for a given plate geometry by varying projectile mass and diameter.
2. The falling weight strain rates were generally lower than those typical of birdstrike. Strain rates coinciding with the low end of the birdstrike range were only achieved for thin (0.125 inch) plates.
3. The energy versus geometric parameter trends for the air cannon tests were the same as those for the falling weight tests; that is, failure energy increased with increasing plate span, plate thickness, and projectile diameter.
4. Failure energy and percent thickness reduction were found to be nonlinear functions of projectile velocity (and thus projectile mass) for the air cannon test. Falling weight failure energy and percent thickness reduction did not depend on projectile velocity or mass.
5. The air cannon test technique achieved the required failure energy for all geometries of specimens. The falling weight test achieved the required failure energy for all but very

thick (0.75 inch) plates, for which drop height and impactor weight maximum limits were insufficient to cause failure.

6. For the air cannon test, onset of specimen failure occurred most often as the ballistic limit, rather than the threshold of failure. Threshold of failure was achieved regularly with the falling weight test.

7. The test data (both air cannon and falling weight) indicated that the ratio of projectile diameter to plate thickness determined the specimen failure mode. For identical test geometries, air cannon failure modes were the same as the falling weight failure modes, with one exception.

SECTION 5

RECOMMENDATIONS

The following are recommended as a result of this investigation.

1. Based on the test data reported herein, the air cannon test technique should be used for impact resistance screening of polycarbonate sheet whenever obtaining strain rates characteristic of birdstrike is deemed critical (and specimen thicknesses exceed 0.125 inch; see Conclusion 2). The falling weight test method should be used for polycarbonate impact resistance screening whenever strain rate is considered to be of lesser importance, since good qualitative results can be obtained and test and maintenance costs are low compared to the air cannon technique. However, it may be necessary to use the air cannon technique to screen very thick (0.75 inch) specimens if failure cannot be achieved by the falling weight technique. (An alternative would be to use beams rather than plates for thickness greater than 0.5 inches.)
2. If air cannon testing is to become a requirement, then it is recommended that an ASTM standard test method be developed. Such a test method would provide testing guidelines which would properly account for velocity-dependent behavior so that meaningful test results are ensured.
3. If Recommendation 2 is pursued, then additional air cannon testing should be performed to:
 - a. Determine the effects of projectile velocity (mass) on failure energy versus plate thickness and projectile diameter;

b. Determine the failure energy of thick (0.5 inch) plates of various spans at very high projectile velocity (projectile mass of 30g), in order to complete the energy versus projectile velocity curves presented in this report;

c. Verify that ballistic limit energies are approximately the same as threshold of failure energies; and

d. Better define the ratios of projectile diameter to plate thickness at which plate failures transition from one failure mode to another (falling weight tests would also be suitable).

4. Review films and literature to better document strain rates for transparencies subject to birdstrike.

REFERENCES

1. ASTM F736-81, "Standard Practice for Impact Resistance of Monolithic Polycarbonate Sheet by Means of a Falling Weight," October 1981.
2. Kenneth I. Clayton, Gregory J. Stenger, Blaine S. West, and Paul E. Johnson, "Development of an Impact Resistant Test Method for Polycarbonate," AFWAL-TR-83-3128, Wright-Patterson Air Force Base, February 1984.
3. G. F. Rhodes, "Damping, Static, Dynamic, and Impact Characteristics of Laminated Beams Typical of Windshield Construction," AFFDL-TR-76-156, December 1977, pp. 7, 246.
4. F. E. Greene, "Testing for Mechanical Properties of Monolithic and Laminated Polycarbonate Materials, Part 1, Test Results and Analysis," AFFDL-TR-77-96 Part 1, Wright-Patterson Air Force Base, October 1978.
5. Marvin E. Backman, Terminal Ballistics, NWC TP 5780, Naval Weapons Center, China Lake, CA., February 1976, pp. 71-76.
6. M. J. Forrestal, Z. Rosenberg, V. K. Luk, and S. J. Bless, "Perforation of Aluminum Plates with Conical-Nosed Rods," SAND 86-0292J, p 2.
7. B. Landkof and W. Goldsmith, "Petalling of Thin, Metallic Plates During Penetration by Cylindro-Conical Projectiles," Int. J. Solids Structures, Vol. 21, No. 3, pp. 245-266, 1985.
8. Joshua Liss and Werner Goldsmith, "Plate Perforation Phenomena Due to Normal Impact by Blunt Cylinders," Int. J. Impact Engng., Vol. 2, No. 1, pp. 37-64, 1984.
9. Raymond J. Roark and Warren C. Young, Formulas for Stress and Strain, Fifth Edition, New York: McGraw Hill Book Company, 1982.
10. "Impact Physics Facilities at the University of Dayton Research Institute," UDR-TM-80-04, September 1982.

•
-
•

APPENDIX A
COMPUTATION OF SPECIMEN STRAIN RATES

A. INTRODUCTION

In-plane strain rates are computed for the tension surface of polycarbonate plate specimens tested by either the air cannon or falling weight technique. The strain rates are computed from measured values of projectile velocity and specimen strain. The computed strain rates are time-averaged values (over the duration of the impact event) rather than instantaneous values.

B. NOMENCLATURE

<u>Variable</u>	<u>Units</u>	<u>Description</u>
a	in	Radius of circular plate
b	in	Side length of square plate
d	in	Forward travel distance of projectile after impact
d_p	in	Total plastic deflection of plate
e	in	Total elastic deformation of plate
E	psi	Plate tensile elastic modulus
h	in	Height of deformed plate
l	in	In-plane deformed length
l_o	in	In-plane length prior to deformation
r_o	in	Projectile radius
r_o'	in	Modified projectile radius (see note below)
t	in	Plate thickness after impact
T	sec	Duration of impact
v	in/sec	Projectile velocity
α	-	Constant for square plate calculations
β	-	Constant for square plate calculations
ϵ	in/in	Total in-plane strain
ϵ_e	in/in	In-plane elastic strain
ϵ_p	in/in	In-plane plastic strain
$\dot{\epsilon}$	in/in/sec	In-plane strain rate

σ_r	psi	Radial normal stress
σ_θ	psi	Tangential normal stress
σ_z	psi	Thickness normal stress
σ_x	psi	x-direction normal stress
σ_y	psi	y-direction normal stress
σ_Y	psi	Yield stress of plate
ν	-	Poisson's ratio of plate

NOTE:

$$\text{For } r_o > 0.5 t_o, r'_o = r_o$$

$$r_o < 0.5 t_o, r'_o = \sqrt{1.6r_o^2 + t^2} - .675t$$

C. STRAIN RATE DERIVATION

1. General Strain Rate Equation

The strain rate is given by

$$\dot{\epsilon} = \epsilon/T \quad (1)$$

where ϵ = the total strain (sum of elastic and plastic strains, ϵ_e and ϵ_p), and
 T = elapsed time from instant of impact to stop of forward projectile motion.

The strain rates are therefore time averaged over the duration of impact.

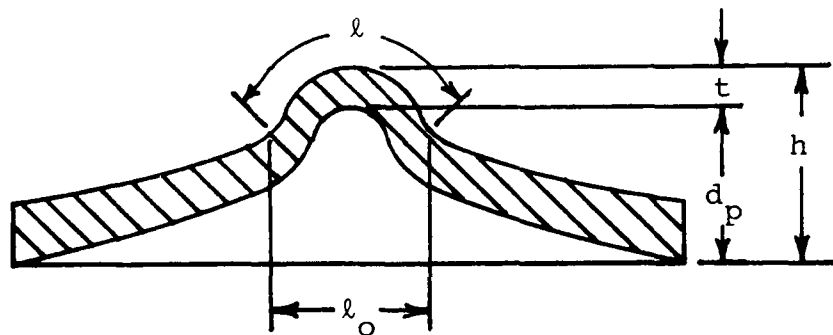


Figure A.1. Specimen Measurements for Computation of Strain Rates.

2. Elastic Strain Computation

The elastic strains are computed from the Hookean constitutive equation

$$\epsilon_e = (\sigma_r - \nu\sigma_\theta - \nu\sigma_z)/E \quad (2)$$

(Note that for square plates, σ_x and σ_y replace σ_r and σ_θ .) Neglect thickness (z-direction) effects, so that $\sigma_z=0$. Also note that, for circular plates subjected to central transverse loading, $\sigma_r=\sigma_\theta$. Finally, note that, for all the plates tested in this program, permanent overall bending deformation was present, meaning that all plates experienced the maximum possible elastic bending deformation when impacted. In other words, $\sigma_r=\sigma_\theta=\sigma_y$ (likewise, $\sigma_x=\sigma_y=\sigma_y$). Equation 2 thus becomes

$$\epsilon_e = (1-\nu) \sigma_y/E \quad (3)$$

3. Plastic Strain Computation

The plastic strain was computed from measurements taken from tested specimens using the equation

$$\epsilon_p = (l - l_0)/l_0 \quad (4)$$

Figure A.1 shows the definitions of l and l_0 . Measurements were made on one specimen from each group, namely, the one that had the highest absorbed energy without failure (ductile deformation only).

4. Duration of Impact Computation

The duration of impact, T , was computed from

$$T = d/(\frac{1}{2}v) \quad (5)$$

where d = distance traveled by projectile from moment of impact to stop of forward motion, and
 v = impact velocity

The average velocity ($\frac{1}{2}v$) is used (initial velocity is v , final velocity is zero, average velocity is $\frac{1}{2}(v+0)=\frac{1}{2}v$).

The distance of projectile travel, d , consists of overall elastic deflection, overall plastic deflection, and local plastic deflection. The overall and local plastic deflections were

computed from measurements taken from tested specimens using the equation

$$d_p = h - t \quad (6)$$

where d_p is the total plastic deflection (overall plus local) and h and t^p are measured as shown in Figure A.1. The elastic deflection, e , is computed using handbook linear elastic, isotropic plate formulas, noting that the elastic limit is attained. Equation 5 thus becomes

$$T = 2(e+h-t)/v \quad (7)$$

The formulas for e vary depending on shape (circular or square) and boundary conditions (clamped or simply supported). Summary formulas based on Roark⁹ are presented:

a. Clamped, Circular plate

From Reference 9, Case 16, p. 366, combining equations for flexural rigidity, moment, and deflection gives

$$e = \frac{\sigma_y a^2 (1-\nu)}{2E t \ln(\frac{a}{r_o})} \quad (8)$$

b. Simply Supported Circular Plate

From Reference 9, Case 17, p. 367, combining equations for flexural rigidity, moment, and deflection gives

$$e = \frac{\sigma_y a^2 (3+\nu)(1-\nu)}{2Et[(1+\nu) \ln(\frac{a}{r_o})+1]} \quad (9)$$

c. Square Plate, All Edges Clamped

From Reference 9, Case 8b, p. 393, combining equations for stress and deflection gives

$$e = \frac{2\pi \alpha b^2 \sigma_y}{3Et[(1+\nu) \ln(\frac{2b}{\pi r_o})+\beta]} \quad (10)$$

where $\alpha = 0.0611$, $\beta = -0.238$

d. Square Plate, All Edges Simply Supported

From Reference 9, Case 1b, p. 386, combining equations for stress and deflection gives Equation 10 with

$$\alpha = 0.1267, \beta = 0.435$$

5. Specific Strain Rate Equation

Combining Equations 1, 3, 4, and 7 gives

$$\dot{\epsilon} = \frac{v}{2(e+h-t)} \left[\frac{(1-v) \sigma_y}{E} + \frac{l - l_0}{l_0} \right] \quad (11)$$

with the values for e being computed from Equations 8-10. Equation 11 was used for computing the strain rates documented in this report.

6. Material properties

The polycarbonate material properties used in Equations 8-11 were:

$$\begin{aligned} E &= 355,000 \text{ psi} \\ \sigma_y &= 12,059 \text{ psi} \\ \nu &= 0.37 \end{aligned}$$

The properties were high strain rate values obtained from Reference 4.

D. STRAIN RATE RESULTS

Specimen I.D.	e (in)	h (in)	t (in)	v (in/sec)	ℓ (in)	ℓ ₀ (in)	Strain Rate (in/in/sec)
A-2	.607	.93	.266	10080	1.54	1.28	890
B-2	.378	.9	.31	9960	1.5	1.25	1105
C-spare	.062	.94	.231	8556	1.56	1.28	1334
D-5	.083	.93	.272	9264	1.56	1.27	1559
E-7	.165	.92	.25	9540	1.51	1.26	1253
F-7	.247	.82	.4	3264	1.5	1.07	1036
G-6	.123	.84	.082	4788	1.43	1.1	873
H-7	.052	.512	.288	2232	.48	.45	358
I-4	.058	.63	.285	5172	.88	.82	605
J-6	.111	1.14	.197	11328	1.95	1.55	3003
K-4	.083	.99	.208	6276	1.46	1.22	793
L-8	.083	.88	.222	3384	1.38	1.19	413
M-3	.083	.95	.195	3060	1.5	1.25	404
N-4	.141	.93	.280	9456	1.55	1.3	1258
O-5	.1110	1.15	.53	12120	1.7	1.57	865
P-7	.165	.51	.042	1980	.93	.71	518
Q-1	.123	.29	.044	1116	.45	.38	310
R-6	.378	.92	.236	7656	1.43	1.25	596
S-7	.378	1.01	.2	4932	1.52	1.29	413
T-3	.378	.92	.207	3924	1.41	1.23	302
U-4	.165	.95	.207	7284 ¹	1.48	1.26	788
V-6	.165	1.2	.2	4920 ¹	1.49	1.22	514
W-1	.165	.9	.211	3180	1.39	1.2	334
FA-3	.165	1.06	.192	374	1.67	1.4	39
FB-4	.062	1.03	.205	385	1.72	1.43	49
FC-6	.147	.94	.053	341	2.04	1.48	98
FD-3	.052	.67	.204	356	1.01	.92	41
FE-4	.052	.56	.308	334	.6	.56	51
FF	----- NOT TESTED -----						
FG-6	.123	.27	.043	284	.5	.41	98
FH-4	.165	.54	.043	312	.95	.67	104
FI-7	.349	1.18	.062	341	2.57	1.82	50
CC-5	.083	1.02	.209	418	1.77	1.49	49

NOTES:

1. Specimen velocity unknown; average failure velocity for group V used.
2. Insufficient data available to compute strain rates for groups DA and DB.

APPENDIX B

SUMMARY OF AIR CANNON TEST DATA

PROJECTILE					PLATE					
SPECIMEN	TYPE	DIAMETER (in)	MASS (g)	VELOCITY (ft/s)	THICKNESS ^a (in)	SPAN ^b (in)	BOUNDARY CONDITIONS ^c	ENERGY (ft-lb)	FAILURE MODE	PERCENT THICKNESS REDUCTION
A - 1	1	1.0	66.7	873	.5	10	SS	1742	B	--
2				840 ^e				1613	D	41
3				863				1702	B	30
4				830 ^e				1574	D	--
B - 1	1	1.0	66.7	858 ^e	.5	10	C	1682	B	--
2				830 ^e				1574	D	31
3				840				1613	B	53
4				826				1559	D	--
C - 1	1	1.0	66.7	838	.5	4	C	1605	B	--
2				835				1593	B	--
3				817				1526	B	--
4				787				1416	B	--
5				759				1317	B	--
6				699				1117	D	--
7				749				1282	B	44
8				713				1162	D	49
D - 1	1	1.0	66.7	855	.5	5	C	1671	B	--
2				795				1444	FB	28
3				793				1436	FB	--
4				781				1394	FB	42
5				772				1362	D	40
6				773				1366	D	--
7				764				1299	D	--
E - 1	1	1.0	66.7	835	.5	8	C	1593	B	--
2				821				1540	B	--
3				787				1416	D	--
4				809				1496	FB	--
5				793				1437	D	--
6				795				1444	B	38
7				795				1444	D	44

PROJECTILE					PLATE					
SPECIMEN	TYPE	DIAMETER (in)	MASS (g)	VELOCITY (ft/s)	THICKNESS ^a (in)	SPAN ^b (in)	BOUNDARY CONDITIONS ^c	ENERGY (ft-lb)	FAILURE MODE	PERCENT THICKNESS REDUCTION
F - 1	1	1.0	66.7	423	.125	4	C	409	T	--
2				310				220	FT	59
3				288				190	FT	63
4				229				120	D	--
5				245				137	D	--
6				255				149	D	--
7				272				169	D	65
G - 1	1	1.0	66.7	461	.25	4	C	486	B	--
2				341				266	D	--
3				369				311	D	--
4				435				432	B	--
5				412				388	B	47
6				399				364	D	64
7				414				392	FB	50
H - 1	2	.25	66.7	S/B ^f	.5	5	C	S/B	S/B	S/B
2				S/B				S/B	S/B	S/B
3				486				550	B	--
4				268				167	FB	--
5				230				123	FB	72
6				200				93	FB	72
7				186				80	D	36
I - 1	3	.5	66.7	560	.5	5	C	718	B	--
2				515				607	B	--
3				478				523	FB	--
4				431				425	D	37
5				466				497	FB	--
6				443				449	B	67
7				441				445	FB	52

PROJECTILE					PLATE			ENERGY (ft-lb)	FAILURE MODE	PERCENT THICKNESS REDUCTION
SPECIMEN	TYPE	DIAMETER (in)	MASS (g)	VELOCITY (ft/s)	THICKNESS ^a (in)	SPAN ^b (in)	BOUNDARY CONDITIONS ^c			
J - 1	4	1.5	66.7	684	.5	5	C	1030	D	--
2				779				1334	D	--
3				813				1453	D	--
4				880				1701	D	--
5				920				1860	D	--
6				944				1961	D	56
7				1065				2496	B	--
8				1018				2270	B	--
9				979				2100	B	49
K - 1	5	1.0	125.6	445	.5	5	C	851	D	--
2				659				1867	B	--
3				618				1642	B	--
4				523				1176	D	54
5				566				1377	B	--
6				553				1315	FB	53
7				531				1218	FB	58
L - 1	6	1.0	289.8	S/B	.5	5	C	S/B	S/B	S/B
2				S/B				S/B	S/B	S/B
3				445				1964	B	--
4				400				1587	B	52
5				321				1022	FB	58
6				253				636	D	35
7				282				790	D	--
8				282				790	D	--
M - 1	7	1.0	402.5	385	.5	5	C	2042	B	--
2				341				1602	B	--
3				255				896	D	57
4				291				1167	B	--
5				261				939	FB	55
6				260				931	FB	62
7				246				834	D	--

P R O J E C T I L E					P L A T E					
SPECIMEN	TYPE	DIAMETER (in)	MASS (g)	VELOCITY (ft/s)	THICKNESS ^a (in)	SPAN ^b (in)	BOUNDARY CONDITIONS ^c	ENERGY (ft-lb)	FAILURE MODE	PERCENT THICKNESS REDUCTION
N - 1	1	1.0	66.7	1070	.5	5	SS	2375	B	--
2				739				1247	D	--
3				892				1817	B	--
4				788				1418	D	38
5				843				1623	B	--
6				817				1524	B	24
0 - 1	1	1.0	66.7	1006	.75	8	C	2311	FB	22
2				956				2087	D	--
3				994				2256	D	34
4				1081				2668	B	--
5				1010				2329	D	--
6				1026				2403	B	--
7				1012				2338	B	38
P - 1	3	.5	66.7	207	.125	4	C	98	B	--
2				155				55	D	--
3				183				77	B	--
4				167				64	FB	61
5				164				62	FB	63
6				158				57	D	--
7				165				62	D	63
Q - 1	2	.25	66.7	93	.125	4	C	20	D	62
2				126				37	FB	--
3				108				27	FB	--
4				100				23	FB	61
5				94				20	FB	60
6				85				17	D	--
7				89				18	D	--

PROJECTILE					PLATE					
SPECIMEN	TYPE	DIAMETER (in)	MASS (g)	VELOCITY (ft/s)	THICKNESS ^a (in)	SPAN ^b (in)	BOUNDARY CONDITIONS ^c	ENERGY (ft-lb)	FAILURE MODE	PERCENT THICKNESS REDUCTION
R - 1	5	1.0	125.6	615	.5	10	C	1620	D	--
2				634				1722	D	--
3				652				1821	B	54
4				630				1700	S/B	S/B
5				630				1700	D	--
6				638				1744	D	48
7				634				1722	B	--
S - 1	6	1.0	289.8	446	.5	10	C	1966	B	--
2				405				1621	D	--
3				407				1637	D	--
4				442				1931	B	--
5				S/B				S/B	S/B	--
6				433				1853	B	47
7				411				1670	D	56
T - 1	7	1.0	402.5	314	.5	10	C	1354	D	--
2				365				1829	B	--
3				327				1468	D	54
4				333				1522	S/B	--
5				343				1615	B	63
6				324				1441	S/B	--
7				363				1809	FB	--
U - 1	5	1.0	125.6	605	.5	8	C	1568	D	--
2				628				1690	B	--
3				602				1553	D	--
4				607				1578	D	54
5				599				1537	D	--
6				627				1684	B	--
7				620				1607	B	44

PROJECTILE				PLATE				ENERGY (ft-lb)	FAILURE MODE ^b	PERCENT THICKNESS REDUCTION
SPECIMEN	TYPE	DIAMETER (in)	MASS (g)	VELOCITY (ft/s)	THICKNESS ^a (in)	SPAN ^b (in)	BOUNDARY CONDITIONS ^c			
V - 1	6	1.0	289.8	291	.5	8	C	837	D	--
2				394				1534	D	--
3				451				2010	B	--
4				412				1678	FB	56
5				430				1828	B	--
6				S/8				S/B	D	--
7				414				1694		56
W - 1	7	1.0	402.5	265	.5	8	C	964	D	53
2				296				1203	FB	52
3				244				817	D	--
4				319				1397	FB	56
5				337				1559	B	--
6				338				S/B	S/B	--
7				319				1397	B	51

NOTES:

^a Nominal thicknesses given. Actual thicknesses are:

Nominal (in)	Actual (in)
.125	.115
.25	.225
.5	.45
.75	.81

^b All values are diameters of circular openings except those of "10", which equal the side of 10" x 10" square opening.

^c SS = Simply supported, C = clamped (all edges).

^d D = Ductile (no penetration), F = Failure (ballistic limit), B = Bending (petalling), T = tensile (cupping).

^e Velocity estimated

^f S/B = Shot bad

APPENDIX C

SUMMARY OF FALLING WEIGHT TEST DATA

SPECIMEN	P R O J E C T I L E			THICKNESS (in)	SPAN (in)	BOUNDARY CONDITIONS	ENERGY (ft-lb)	FAILURE MODE	PERCENT THICKNESS REDUCTION
	DIAMETER (in)	MASS (lb)	HEIGHT (ft)						
FA - 1	1.0	60.22	14.0	.5	8	C	843	D	--
2		60.57	15.0				909	D	--
3		60.57	15.04				911	D	57
4		60.57	16.0				969	B	--
5		60.57	15.5				939	B	--
6		60.57	15.25				924	B	--
7		60.57	15.06				912	B	54
FB - 1	1.0	52.16	15.0	.5	4	C	782	F	--
2		52.52	14.89				782	D	--
3		52.52	15.5				814	D	--
4		52.52	16.0				840	D	54
5		52.52	18.0				945	B	--
6		57.45	15.5				890	B	60
7		41.91	20.0				838	D	--
FC - 1	1.0	14.03	12.0	.125	4	C	168	n	--
2			12.47				175	D/B	D/B
3			13.0				182	T	--
4			12.47				175	D	--
5			12.69				178	T	--
6			12.54				176	D	54
7			12.58				177	T	55
FD - 1	.5	9.08	11.0	.5	5	C	100	D	--
2		17.02	11.75				200	D	--
3		21.97	13.65				300	D	55
4		26.92	14.86				400	B	--
5		26.92	12.5				337	B	--
6		26.92	11.5				310	B	--
7		26.92	11.25				303	B	57

SPECIMEN	P R O J E C T I L E			THICKNESS (in)	SPAN (in)	BOUNDARY CONDITIONS	ENERGY (ft-lb)	FAILURE MODE	PERCENT THICKNESS REDUCTION
	DIAMETER (in)	MASS (lb)	HEIGHT (ft)						
FE - 1	.25	8.94	11.19	.5	5	C	100.0	S	--
2		8.94	10.0				89.4	S	31
3		6.89	11.0				76.8	D	--
4		6.89	12.0				82.7	D	32
5		6.89	12.5				86.1	S	33
6		6.89	12.17				83.8	S	24
7		6.89	12.08				83.3	S	42
FF			Not Tested - Required Energy Exceeded Apparatus Capability						
FG - 1	.25	2.2	9.0	.125	4	C	19.8	B	--
2			8.0				17.6	D	--
3			8.5				18.7	D	--
4			8.75				19.3	B	61
5			8.58				18.9	D	--
6			8.67				19.1	D	63
7			8.7				19.2	F	57
FH - 1	.5	5.24	10.0	.125	4	C	52.4	F	63
2			9.5				49.8	D	--
3			10.25				53.7	D	--
4			10.5				55.1	D	63
5			12.0				62.9	BT	--
6			11.0				57.6	BT	--
7			10.67				55.9	T	62
FI - 1	1.5	33.8	10.0	.125	4	C	338	T	--
2		23.4	8.0				187	D	--
3		23.4	9.0				211	D	--
4		23.4	11.0				257	D	--
5		23.4	13.0				304	T	45
6		23.4	12.0				281	D	--
7		23.4	12.5				293	D	46